UNIVERSITY OF MINNESOTA

This is to certify that I have examined this copy of a master's thesis by

Sally Kay Goodman

and have found it is complete and satisfactory in all respects,
and that any and all revisions required by the final
examining committee have been made.

Dr. Vicki Hansen

_____

Name of Faculty Advisor

_____

Signature of Faculty Advisor

_____

Date

GRADUATE SCHOOL

Structural and Kinematic Analysis of the Kawishiwi Shear Zone, Superior Province: Insight on Granite-Greenstone Terrain Tectonics and Archean (2.7 Ga) Crustal Evolution

A THESIS
SUBMITTED TO THE FACULTY OF THE GRADUATE SCHOOL
OF THE UNIVERSITY OF MINNESOTA
BY

Sally Kay Goodman

IN PARTIAL FULFILLMENT OF THE REQUIREMENTS
FOR THE DEGREE OF
MASTER OF SCIENCE

Dr. Vicki Hansen

September 2008

Acknowledgements

I would like to thank the following organizations and people for making this work possible:

For Funding Support:
- Student Research Grants:
  Precambrian Research Center
  Geological Society of America
  Institute on Lake Superior Geology
  UMD Geological Sciences Department
- University of Minnesota Grant-in-Aid through support granted to J. Goodge
- McKnight Foundation through support granted to V.L. Hansen by the McKnight Presidential Endowment
- National Science Foundation GK-12 fellowship program for tuition and salary

People:
- Dr. Vicki Hansen, advisor
- Committee: Dr. Scott Freundschuh, Dr. John Goodge, Dr. Nigel Wattrus
- GIS support: Matt Goodman, Stacey Stark
- Field Assistant: Amanda Putz
- USFS: allowance of sample collection in BWCAW
- Vancouver Petrographic: Petrographic thin section preparation
- John Schiefelbein, North Country Canoe Outfitters:
  for use of 2 Duluth Packs and their geologic curiosity
- Rick Allmendinger: for *Stereonet 6.3.3* freeware
- Dr. John Green: for his work in the Kawishiwi River Region
- The Shear Zone Gals: Emerald Erickson, Susie Karberg, Jenny Koester
- Fellow graduate students for all levels of feedback and support
- Family, especially my husband Matt: for their support and curiosity

Dedication

This thesis is dedicated to children who already know that Earth is old; may they remember as much and learn to understand.

Abstract

Two conflicting hypotheses have been invoked to explain the formation of Archean (~2.7 Ga) granite-greenstone terrains: 1) granite-greenstone terrains represent collapsed back-arc or sutured forearc basins of subduction-driven accreted terranes, and 2) granite-greenstone terrains formed by density-driven sagduction of an insulating greenstone cover and concurrent rising of granite diapirs. Granite-greenstone terrains commonly preserve shear zones, which record critical clues to Archean crustal evolution processes.

A structural and kinematic analysis of the Kawishiwi Shear Zone (KSZ), within the Vermilion District of the Superior Province, was conducted to evaluate the tectonic processes of granite-greenstone formation. The KSZ, broadly bounded by the Vermilion Granitic Complex to the north and the Giants Range Batholith to the south forms one of several east-northeast striking, steeply-dipping shear zones in the Vermilion District. Foliated and lineated rocks (L-S tectonites) generally record greenschist and amphibolite facies metamorphism. The ca. 30 km KSZ length is truncated by the north-striking Waasa fault in the west and younger (1.1 Ga) Keeweenawan intrusive rocks in the southeast. Locally, the KSZ cuts rocks of the Ely Greenstone, Knife Lake Group (graywacke, tuff, conglomerate, and felsic to intermediate volcanic rocks), and the Giants Range granitoid.

In order to understand the KSZ kinematic and structural evolution, major data collection and analysis included: 1) metamorphic foliation (Fm), mineral elongation lineation (Le) and pitch domains from field mapping the eastern 24 km by 10 km KSZ, and existing geologic maps; 2) outcrop-scale and microstructural kinematic analysis from oriented rock samples; 3) quartz c-axis petrographic fabric analysis; and 4) general metamorphic history from lithology and thin section petrography.

The ~3-5 km wide and steeply dipping (~075, 90) KSZ, hosts bimodal Le, with dominant steeply-plunging Le and local gently-plunging Le. I collected 127 oriented samples, and cut 35 samples for 55 thin sections. Of these, 20 samples (represented by

33 thin sections) had discernible asymmetric fabrics within the L-S tectonite motion plane. Of these 20, 16 display dip-slip Le and 4 display strike-slip Le. Asymmetric fabrics occur in Fm-perpendicular, Le-parallel planes and symmetric fabrics occur in Fm-perpendicular, Le-perpendicular planes. Therefore, Le lies parallel to the motion plane or vorticity normal section, which is consistent with non-coaxial shear with *lineation forming parallel to shearing*. It follows that in high pitch domains, displacement was vertical to oblique; microstructures record both north-side-up and south-side-up displacement in different samples. Within the shallow pitch domain, shear sense indicators consistently record dextral strike-slip displacement.

Three samples were analyzed for quartz petrofabric (two from dip-slip Le and one from strike-slip Le). Two of three quartz c-axis analysis results show basal slip was operative during deformation, consistent with greenschist and lower amphibolite metamorphic facies results. One quartz c-axis sample is interpreted to have a 2-stage deformation history. Quartz c-axes fabrics record activation of the rhombohedral slip system indicating higher-than-amphibolite facies T during deformation. However, the c-axis fabric more likely results from early dip-slip shear creating a low-T c-axis orientation followed by dextral strike-slip shear re-orienting the c-axes to an apparent medium-T orientation of rhombohedral slip, an interpretation consistent with kinematic analysis of the KSZ.

The structural and kinematic results point to at least two shearing events in the KSZ: and early distributed ductile dip-slip shear, and a subsequent, more localized dextral strike-slip shear. Curving Fm trajectories in the Giants Range granitoid, distributed and dominant dip-slip shear and later strike-slip shear favors the sagduction-diapirism hypothesis whereby a high Archean geotherm dictates widespread density-driven ductile deformation of rising granites and sinking greenstone/sediment packages.

Table of Contents

List of Tables

Page

In Text:

Appendix:

Oversize Plates:

List of Figures

Page

In Text:

Oversize Plates:

List of Abbreviations

In-Text Abbreviations

Boundary Waters Canoe Area Wilderness	BWCAW
electron backscatter diffraction	EBSD
elongation lineation	Le
grain-shape preferred orientation	GSPO
Kawishiwi Shear Zone	KSZ
lattice-preferred orienation	LPO
lineated and foliated rock	L-S tectonite
metamorphic foliation	Fm
Minnesota Geological Survey	MNGS
pressure-temperature	P-T
Universal-stage microscope	U-stage

Mineral Abbreviations

Actinolite	Act
Albite	Ab
Amphibole	Amp
Apatite	Ap
Biotite	Bt
Calcite	Cal
Chlorite	Chl
Clinozoisite	Czo
Dolomite	Dol
Epidote	Ep
Feldspar	Fsp
Grunerite	Gru
Hornblende	Hbl
Orthoamphibole	Oam
Iron Oxide	Fe-o
Plagioclase	Plag
Potassium Feldspar	Kfsp
Pyrophyllite	Prh
Pyrite	Py
Quartz	Qtz
Scaprolite	Scp
Spinel	Spn
White Mica	WhM
Zircon	Zrc

1. Introduction

By the Archean (3.8-2.50 Ga), some form of tectonic processes operated on Earth, yet debate about the nature of tectonic processes that formed one major Archean terrain type, granite-greenstone terrains, still rages (Maufe et al., 1919; Macgregor, 1951; Anhaeusser et al., 1969; Sims, 1976; Sims, 1976; Mareschal and West, 1980; Jelsma and van der Beek, 1993; Collins and Van Kranendonk, 1998; Dalstra et al., 1998; Chardon et al., 2002; Bedard et al., 2003; Rey et al., 2003; Van Kranendonk et al., 2004; Lin, 2005; Rey and Houseman, 2006; Card, 1990; Bauer and Bidwell, 1990; Percival and Skulski, 2000; Tabor and Hudleston, 1990; Jirsa et al., 1992; Kimura et al., 1993; Sims et al., 1993; Lin et al., 1996; Mueller et al., 1996; Kusky and Polat, 1998; Czech and Hudleston, 2003; Van Kranendonk, 2004; Cawood, 2006). Granite-greenstone terrains, which occur in every present-day Earth continent typically display a planform pattern of quasi-circular granitic bodies within equant to elongate belts of metavolcanic greenstone and metavolcanic rock packages (Fig. 1). Physical and chemical laws are the key to Archean granite-greenstone terrain formation processes. The structural and kinematic record within granite-greenstone terrains likely records critical clues of granite-greenstone terrain evolution, which in turn provide insight on the crustal evolution on Earth.

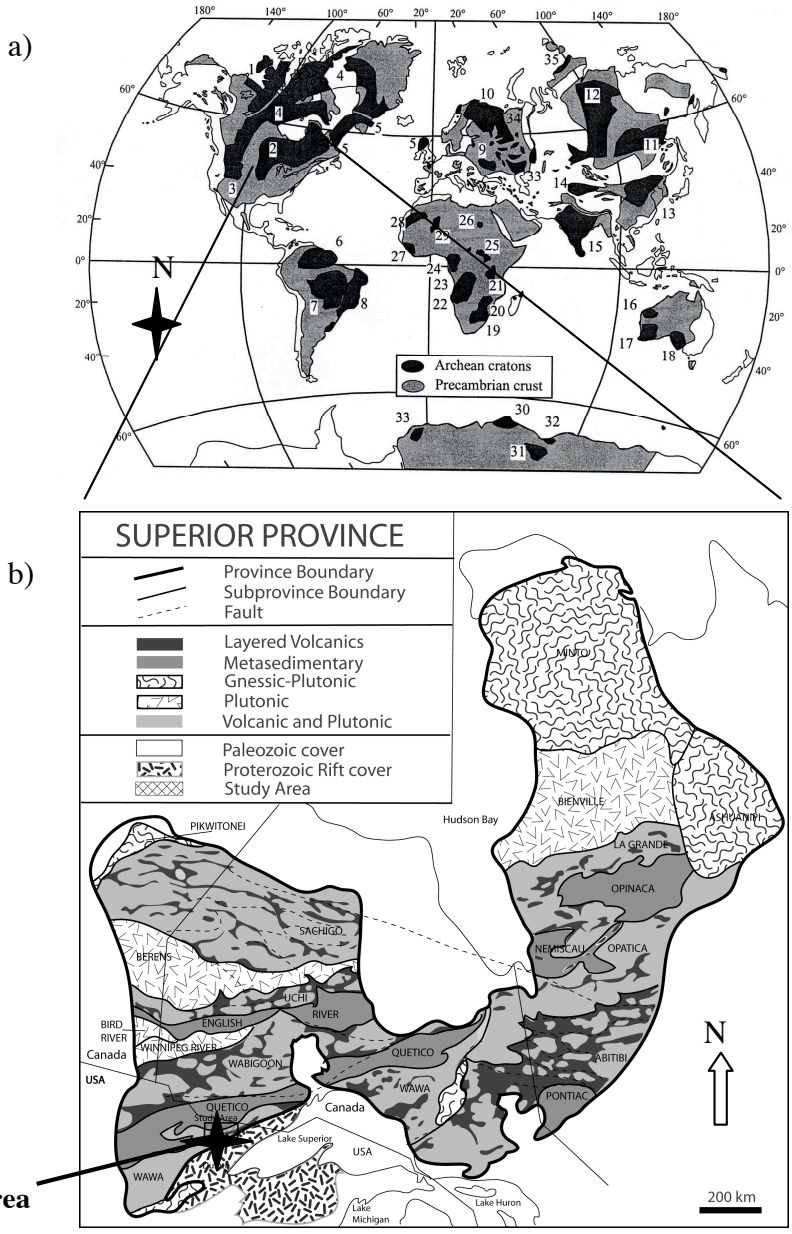

Figure 1. a) Archean cratons and areas underlain by Precambrian crust include the following Cratons/Provinces: 1=Slave, 2=Superior, 3=Wyoming, 4=Kaminak (Hearne), 5=North Atlantic (Nain, Godthaab, Lewisian), 6=Guiana, 7=Central Brazil (Guapore), 8=Atlantic (Sao Francisco), 9=Ukranian, 10=Baltic (Kola), 11=Aldan, 12=Anabar, 13=Sino-Korean, 14=Tarim, 15=Indian, 16=Pilbara, 17=Yilgarn, 18=Gawler, 19=Kaapvaal, 20=Zimbabwe, 21=Zambian, 22=Angolan, 23=Kasai, 24=Gabon, 25=Kibalian, 26=Uweinat, 27=Liberian, 28=Maritanian, 29=Ouzzalian, 30=Napier Complex, 31=Prince Charles Mountains, 32=Vestfold Hills, 33=Heimefront Ranges, 34=deeply buried Archean rocks of East European Shield, 35=Tajmyr. (adapted from Kusky and Polat, 1999). b) The Superior Province and subprovinces form a granite-greenstone terrain (adapted from Card, 1990).

Two hypotheses of granite-greenstone terrain formation garner support: one invokes a Proterozoic- to Phanerozoic-style of subduction-driven, island arc terrane accretion at convergent margins (e.g., Windley, 1984; Stanley, 1992; Kimura et al., 1993); the other, sagduction/diapirism, invokes sinking of dense greenstone cover rocks as buoyant granite domes rise due to gravitational instability (e.g., Anhauesser, 1969; Rey et al., 2003; Van Kranendonk et al., 2003) (Figs. 4 and 5). Many interpretations of the Superior Province of North America (assembled roughly from 3.1 to 2.5 Ga), favor arc-accretion hypothesis (Card, 1990; Bauer and Bidwell, 1990; Percival and Skulski, 2000; Tabor and Hudleston, 1990; Jirsa et al., 1992; Sims et al., 1993; Lin et al., 1996; Mueller et al., 1996; Kusky and Polat, 1998; Czech and Hudleston, 2003; Cawood, 2006). Other granite-greenstone terrain interpretations invoke the sagduction/diapirism hypothesis for granite-greenstone terrain formation in the Superior Province (Macgregor, 1951; Sims, 1976; Bedard et al., 2003; Lin, 2005) and other Archean provinces (Maufe et al., 1919; Macgregor, 1951; Anhaeusser et al., 1969; Mareschal and West, 1979; Collins and Van Kranendonk, 1998; Chardon et al., 2002; Rey et al., 2003; Van Kranendonk et al., 2004; Rey and Houseman, 2006).

Faults and shear zones record aspects of regional deformation. Shear zones accommodate and record the relative displacement of the adjacent rock packages within ductile deformation zones, whereas faults accommodate displacement as planes in brittle materials. The Kawishiwi Shear Zone (herein referred to as KSZ, not to be confused with the Kapaskasing Structural Zone) of northeastern Minnesota, U.S.A. warrants such study (Figs. 2 and 3). The KSZ, broadly bounded by the Vermilion Granitic Complex to

the north and the Giants Range Batholith (hereafter referred to as the Giants Range granite body or granitoid) to the south forms one of several east-northeast-striking, steeply-dipping shear zones in the Vermilion District of the Wawa Subprovince of the Superior Province. The ca. 30 km long KSZ is truncated by the north-striking Waasa fault in the west and younger (1.1 Ga) Keeweenawan intrusive rocks in the southeast. Locally, the KSZ lies within the Ely Greenstone, Knife Lake Group (graywacke, tuff, conglomerate, and felsic to intermediate meta-volcanic rocks), and the Giants Range granite body (Fig. 2). A structural and kinematic analysis of the KSZ was conducted to understand its deformation history, which might in turn be used to re-evaluate the two hypotheses on the formation of granite-greenstone terrains.

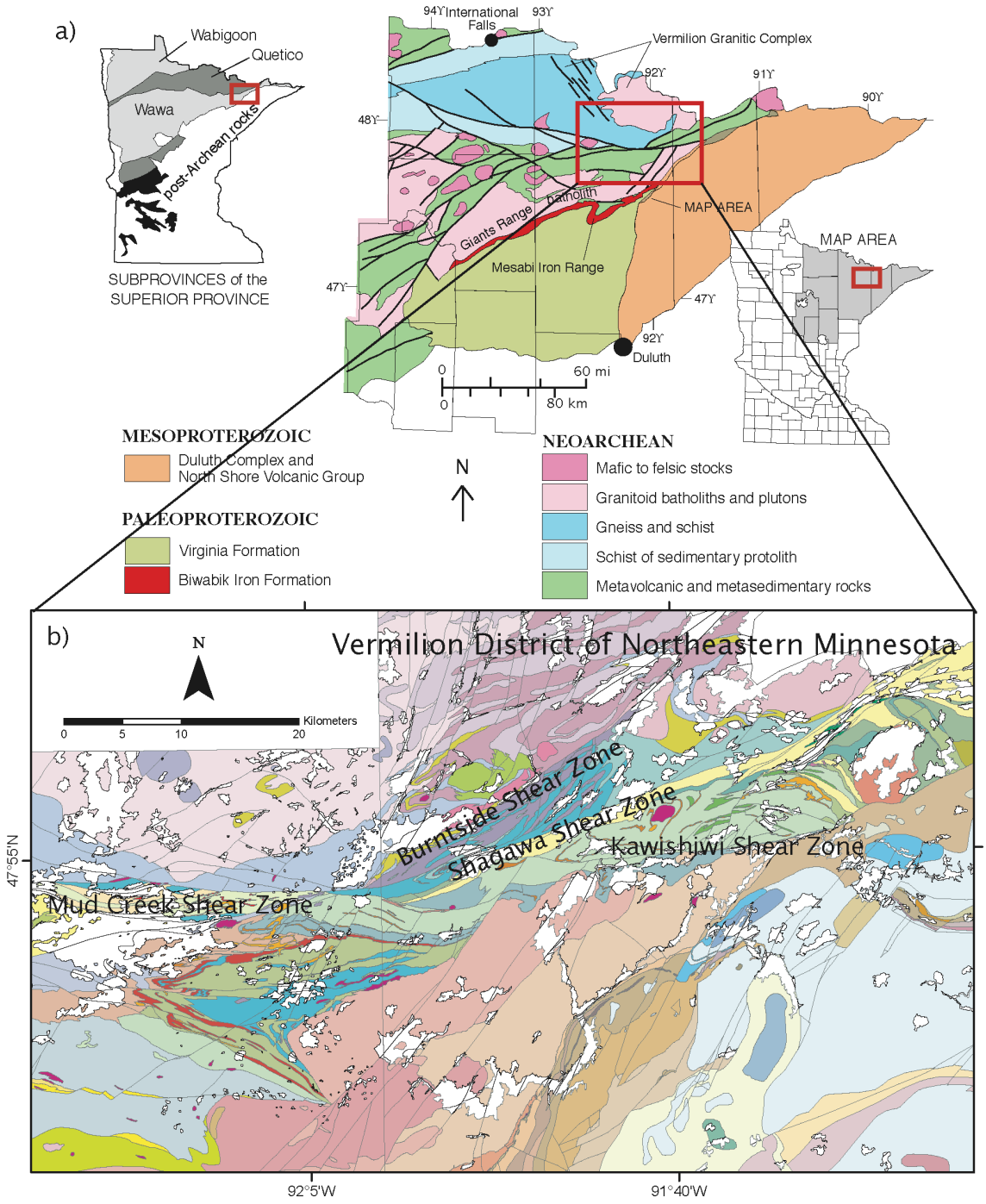

Figure 2. a) Generalized Minnesota Precambrian geology and Vermilion District location. b) Shear zones of the Vermilion District and location of the KSZ. (from Jirsa and Boerboom, 2003; Jirsa and Miller, 2004)

The purpose of this study is to determine the structural and kinematic history of the KSZ and to re-evaluate the conflicting arc-accretion and sagduction/diapirism hypotheses in light of that history. The deformation history of the KSZ is largely unknown. In order to decipher the tectonic processes that molded the tract of Archean granite-greenstone terrain crust near and within the KSZ, data collected and interpreted includes: 1) metamorphic facies, 2) metamorphic foliation (Fm), 3) elongation lineation (Le), 4) kinematic shear sense indicators and 5) quartz petrofabric patterns. Herein, I describe: 1) testable three-dimensional structures and metamorphic signatures predicted by the competing hypotheses of arc-accretion and sagduction/diapirism, 2) methods and results of this study, and 3) discussion of new and previously documented data from the Superior Province, data from other granite-greenstone terrains, interpretations thereof, and implications for the two proposed hypotheses.

The important debate between arc-accretion and sagduction/diapirism processes for granite-greenstone terrain formation remains an active one. This debate embraces questions about Earth's early crustal rheology. Granite-greenstone terrain formation marks an integral step in the Earth's crustal evolution. Granite-greenstone terrains also host economically important hydrothermal mineral deposits of iron, zinc, copper, gold, silver, lead, cobalt and occasionally nickel (LaBerge, 1994). More evidence for and/or against the two hypotheses is necessary to interpret the thermo-tectonic evolution of the Archean continental lithosphere, particularly for the Superior Province where current interpretations largely favor the arc-accretion hypothesis, although the data does not necessarily discount the sagduction/diapirism hypothesis. Analysis of the KSZ herein has revealed part of the structural and kinematic history of the KSZ, which has implications

for Archean crustal processes and the sagduction/diapirism and arc-accretion hypotheses for granite-greenstone terrain formation.

2. Background

The processes of early crustal evolution on Earth remain largely unknown, but the structural and kinematic record of Archean granite-greenstone terrains holds at least a partial history of tectonic processes. Variables that affect rheology, particularly the Archean thermal regime, would dictate tectonic processes. Despite a warmer-than-present Archean geotherm, structural and kinematic data may still provide keys to the past. Superior Province granite-greenstone terrain data warrants re-evaluation as interpretations invoke both sagduction/diapirism and arc terrane accretion hypotheses.

2.1 Granite-Greenstone Terrains

Most preserved granite-greenstone terrains, tectonically stable since the Archean, form the cratonic interiors of many continents (Fig. 1a.) (Kusky and Polat, 1998). Granite-greenstone terrains extend for hundreds to thousands of kilometers. In map view, the Superior Craton, approximately 2500 km from east to west and 1500 km from north to south, appears as a boldly striped canvas on which east-northeast bands of gneisses alternate with lenticular granite-greenstone belts where that surround rounded plutons of granitoid bodies (Fig. 1b.). Granite-greenstone terrains include mafic volcanic rocks, pyroclastic materials, lithified sediments, and felsic to intermediate granitoid bodies. Greenstones are fine-grained, weakly metamorphosed, greenschist- to amphibolite-facies, commonly pillowed, basalt lava flows. Chlorite, actinolite, and/or epidote give

greenstones a characteristic greenish hue, and reflect basalt alteration by heated groundwater (LaBerge, 1994). Extensive volcanic and volcaniclastic tuffs, breccias, and other fragmental materials, as well as sedimentary deposits including banded-iron formations, also occur in the greenstone belts. Iron formations, consisting of chert and iron-rich minerals hematite and/or magnetite, and thick accumulations of detrital sedimentary rocks, conglomerate, and graywacke overlie and grade into the volcanic sequences. Near the granitoid bodies greenstones typically record amphibolite metamorphic facies, higher grade than greenstones away from the granitoid margins (e.g., Sims, 1976; Mareschal and West, 1980; Green, 1970; Van Kranendonk et al., 2004).

2.2 Archean Thermal Characteristics

The rheology of most lithologies depends strongly on temperature; therefore, the Archean thermal regime would have controlled, in large part, Archean tectonic and granite-greenstone terrain formation. Long-lived radioactive isotope heat generation in the Archean produced a geothermal gradient two-to-four times greater than the present geothermal gradient (Fowler, 2005 and references therein; Lambert, 1980). In addition, basalt lava flows that cover a radiogenic-rich crust could insulate, and therefore accentuate, the thermal anomaly in underlying granites (Rey et al., 2003). Some authors have suggested that Archean ocean crust generation was faster than today due to more intense mantle convection, and as a result, microplates moved faster and collided more often (Burke and Kidd, 1978; Kimura et al., 1993; Windley, 1984).

Archean granite-greenstone terrain structural features that formed under a high crustal geothermal gradient provide a history of Earth's crustal rheology before 2.5 Ga. A

change of crustal rheology, an apparent relaxing of the geotherm and the consequent crustal stabilization, marks the Archean/Proterozoic boundary. The 2.5 Ga Great Dike of Zimbabwe intrudes into older granite-greenstone terrains, indicating that Earth's crust was more brittle than at any earlier stage (Macgregor, 1951; Jelsma et al., 1993; Bjornerud, 2005). Arguably, the earliest documented subduction-related high-grade metamorphic rocks, Tanzanian eclogites, did not form until 2 Ga (Moller et al., 1995). Archean granite-greenstone terrains therefore, record an important time-step in the evolution of Earth's crust, a time before significant evidence of a brittle tectonic regime appears.

2.3 Granite-Greenstone Terrain Formation Hypotheses

Although several hypotheses have been proposed for granite-greenstone terrain formation (Windley, 1984), two major hypotheses currently dominate: 1) granite-greenstone terrains formed by arc terrane accretion under a modern-like (Phanerozoic-age, 542 Ma—present) plate tectonic regime, or 2) granite-greenstone terrains formed by sagduction of high-density greenstone basins and diapirism of lower density granitic bodies.

2.3.1 Arc Terrane Accretion Hypothesis

What I refer to as the arc terrane accretion hypothesis, or arc-accretion hypothesis, has also been called the "mobilist or plate tectonic" (Windley, 1984), "actualistic model" (Rey, 2002; Chardon et al., 2002), "horizontal tectonics" (Van Kranendonk et al., 2003), and "uniformitarian view" (Kearey and Vine, 1996) of granite-greenstone terrain

formation. In the arc-terrane accretion hypothesis, granite-greenstone terrains originate in a convergent margin setting where subduction begins as abundant and small Archean protocontinents (remnant arcs or oceanic plateaus) converge, and the protocontinents accrete by suturing (Fig. 3). The granite-greenstone terrains form either along subduction zones through offscraping and accretion of oceanic crust or plateaus (Fig. 3) (Stanley, 1992; Kimura et al., 1993; Kusky and Polat, 1999) or in an extended back-arc region, forming narrow basins with igneous sequences fed by mafic dikes intruding through the arc basement (Fig. 3) (Windley, 1984; Kusky and Polat, 1999). Accretionary fore-arc greenstones subsequently deform and slab melts produce granites that intrude the greenstones as continued convergence subjects the back-arc or forearc basin to regional shortening or oblique shortening (transpression) (Kearey and Vine, 1996). Sediments originating from the flanking continent and volcanic arc cover the volcanic sequences, and chert and fine-grained turbidites overlie pillowed lava flows in the center of the fore-arc or back-arc basin. Closure of the back-arc basin forms folds and cleavage in the volcanic-sedimentary packages, and initiates major shear zones in the basement rocks (Kusky and Polat, 1999). The arc-accretion hypothesis embraces the assumption that the high Archean heat flow dissipated through greater ridge activity at longer-than-present ridges and subduction zones drove faster-than-modern accretion of smaller, more numerous continental plates (Windley, 1984; Burke and Kidd, 1978). Structural features similar to those expected in a Phanerozoic convergent setting include: 1) fold-and-thrust belts typical of relatively cold and brittle crust, 2) uniform fold vergence with axial planes and fold axes parallel to the plate boundary, 3) discrete high-strain terrane boundaries marked by strike-slip shear zones and suture zones of accreted terranes, 4)

younging direction by order of accretion, 5) high-P metamorphism from subducted oceanic lithosphere, and 6) uniform orientations of Fm and Le (Table 1).

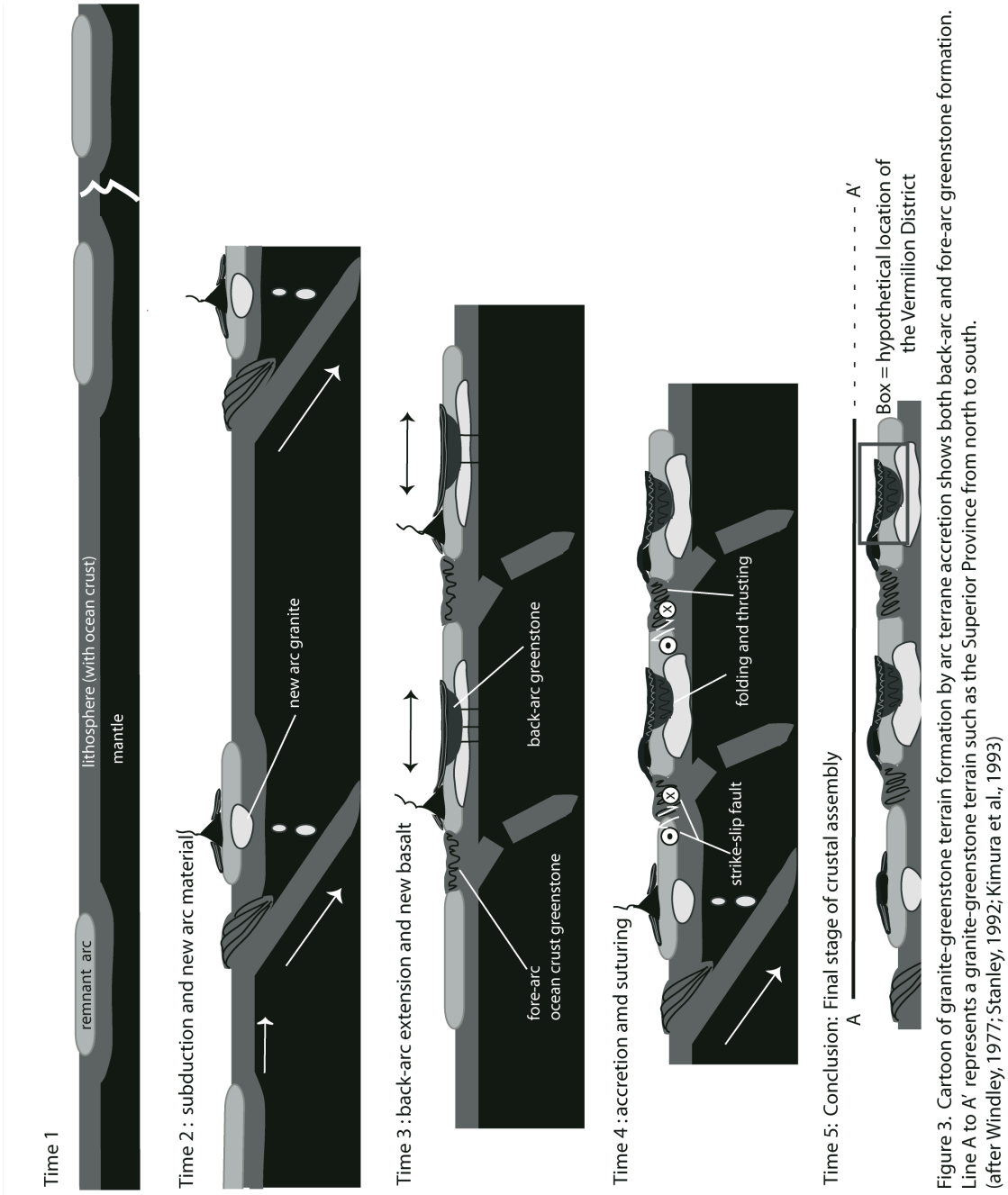

Figure 3. Cartoon of granite-greenstone terrain formation by arc terrane accretion shows both back-arc and fore-arc greenstone formation. Line A to A' represents a granite-greenstone terrain such as the Superior Province from north to south. (after Windley, 1977; Stanley, 1992; Kimura et al., 1993)

2.3.2 *Greenstone Sagduction and Granite Diapirism Hypothesis*

What I refer to as the sagduction/diapirism hypothesis other authors have called "fixist or classical" (Windley, 1984), "vertical tectonics" (Bedard et al., 2003; Van Kranendonk et al., 2003; Lin, 2005), or the "non-uniformitarian view" (Kearey and Vine, 1996) of granite-greenstone terrain formation. In the sagduction/diapirism hypothesis, an early sialic or granitoid crust differentiates from the mantle (Fig. 4, time 1). This granitoid crust contains radiogenic elements that produce heat. Minor thickness variations in the granitoid crust, mantle plumes, and/or pre-existing crustal fractures allow basaltic mantle melt to escape to the surface of the granitoid crust (Anhaeusser et al, 1969) (Fig. 4, times 2-3). Thick volcanic sequences of basalt (commonly subaqueous), pyroclastic flows, and eroded sediments blanket the granitoid crust (Fig. 4, time 3), thermally insulating the underlying granitic crust, softening the underlying granite and possibly inducing partial melting (Mareschal and West, 1980; Rey, 2003). Mantle plumes possibly supply additional heat to the granitic crust. Buoyant and ductile granitoid material, likely still in the solid-state, rises as the denser basalt/pyroclastic/sediment greenstone packages sink (Fig. 4, times 4-5). Volcanic sequences vary from mafic (mantle-derived) to felsic (Lambert, 1980).

Although the sagduction/diapirism granite-greenstone terrain process does not occur today, we can evaluate the hypothesis based on physical and chemical laws that remain constant throughout the life of the universe. The sagduction/diapirism hypothesis predicts: 1) low-grade metamorphism of basalt, with higher grade possible near the granitoid contact surfaces, 2) ranges in Fm orientations that mimic or follow the curving to curvi-linear granitoid/greenstone contacts with steepest Fm occurring near those

contacts, 3) ranges in Le orientation that are steepest in areas with granitoid-up and greenstone-down shear sense, and 4) down-dip shear between sinking and rising crustal domains (Table1).

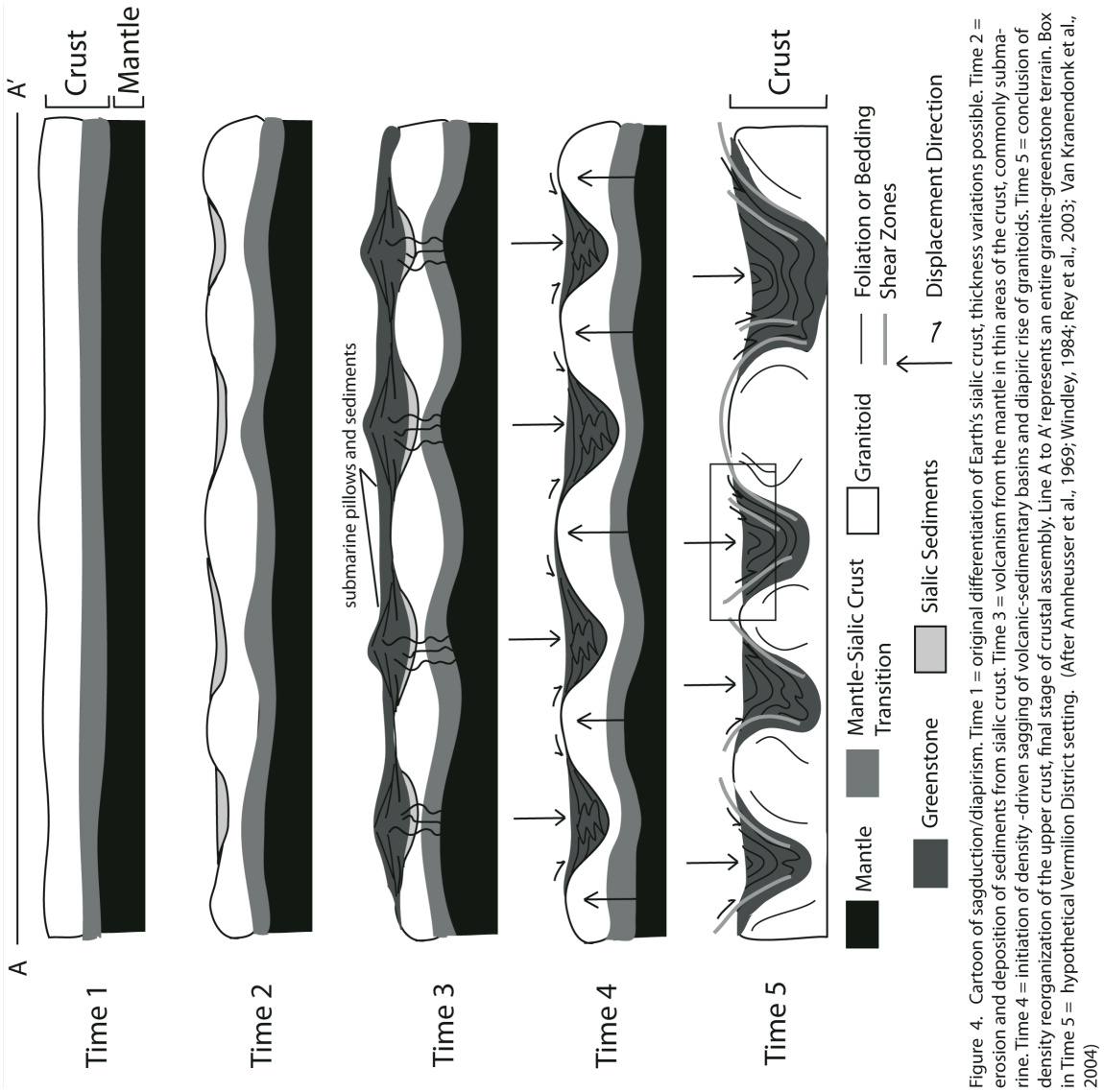

Figure 4. Cartoon of sagduction/diapirism. Time 1 = original differentiation of Earth's sialic crust, thickness variations possible. Time 2 = erosion and deposition of sediments from sialic crust. Time 3 = volcanism from the mantle in thin areas of the crust, commonly submarine. Time 4 = initiation of density -driven sagging of volcanic-sedimentary basins and diapiric rise of granitoids. Time 5 = conclusion of density reorganization of the upper crust, final stage of crustal assembly. Line A to A' represents an entire granite-greenstone terrain. Box in Time 5 = hypothetical Vermilion District setting. (After Annheusser et al., 1969; Windley, 1984; Rey et al., 2003; Van Kranendonk et al., 2004)

Table 1. Hypotheses Predictions

	ARC TERRANE ACCRETION	SAGDUCTION / DIAPIRISM
Strain Distribution	Localized	Distributed
Displacement Directions	Uniform and kinematically tied to Plate boundaries	Various
Metamorphic Foliations (Fm)	Uniform, Planar and kinematically tied to Plate boundaries	Mimic granitoid boundaries
Metamorphic Facies	High P/T to Low P/T	Low P/T to Med P/T
Younging Direction	Consistent younging across order of accretion	No
Fold-and-thrust belts	Likely	Possible
Transpression	Possible	Possible
Overall Crustal Thickening	Yes	No
Horizontal translation at 100's km - scale	Yes	No

2.4 Granite-Greenstone Terrain Observations and Interpretations

Initially, researchers favored the sagduction/diapirism hypothesis (e.g., Maufe, 1919; Macgregor, 1951; Anhaeusser et al., 1969). However, plate tectonic theory (~1967) ushered in a gestalt switch whereby many subsequent researchers favored the arc-accretion hypothesis. At present, neither hypothesis is universally accepted, although many researchers favor an arc-accretion process of granite-greenstone terrain formation for the Superior Province. First-order observations and interpretations of granite-greenstone terrain are critical to this debate, and to our understanding of the Superior Province.

Near the turn of the century, Maufe (1919) described and interpreted the structures near a granite body in a granite-greenstone terrain in Rhodesia (Zimbabwe):

> "It is a general rule…that the strike of the schists and of their foliation is parallel to the edge of the batholiths and to the banding of the gneissic granite. Secondly, the batholiths, being roughly oval bodies, having curving margins, there being no general direction of stike throughout the country independent of the granite batholiths. Thirdly, the schists almost always dip away from the margins of the batholiths, thus appearing to be synclinal areas. These constant relations between the granite batholiths and the structure of the schist belts imply some connexion (sic) between the upwelling of the granite and the folding of the schists. The general structure of the metamorphic areas of Southern Rhodesia thus offers a strong contrast with that of folded regions, such as the Alpine or Caledonian." (Maufe, 1919, in Macgregor, 1951)

Macgregor first interpreted a granite-greenstone terrain in Rhodesia as the result of a succession of "orogenic episodes" with a regional unidirectional stress regime based on a single, almost anecdotal, continuous line of strike of formations. He later (1951) retracted his original interpretation. Noting that his orogenic interpretation ignored the other significant curving strikes of formations and curving foliations, which support a density-driven diapirism model of granitoid emplacement (McGregor, 1951). More recent interpretations of granite-greenstone terrain data hinge on similar observations.

Much recent work in the Superior Province favors the arc terrane accretion hypothesis (e.g., Bauer and Bidwell, 1990; Kimura et al., 1993; Percival and Skulski, 2000; Tabor and Hudleston, 1990; Jirsa et al., 1992; Sims et al., 1993; Lin et al., 1996; Mueller et al., 1996; Hudleston et al., 1998; Kusky and Polat, 1998; Czech and Hudleston, 2003; Cawood, 2006). According to Card (1990) and Cawood (2006) the Superior Province assembled progressively from north to south during multiple discrete orogenic events of oblique accretion of island arcs. Card (1990) and references therein, cite the following sequence of events in the Vermilion district: 1) early deformation resulted in recumbent, nappe-style folds in both the Vermilion greenstone belt and the

adjacent Quetico province; 2) a second polyphase event of N-S shortening and dextral shear with a north-side-up component of displacement accompanied by low-grade metamorphism produced upright, moderately to steeply plunging folds with axial planar foliation and steep lineations; 3) late, increasingly brittle, deformation led to further folding and formation of kink bands, local shear zones, and dextral faults. The Rocas Verdes (green rocks) complex in Southern Chile, formed in the back-arc of a convergent margin setting, is the most similar modern equivalent of Archean granite-greenstone terrains according to Tarney et al. (1976) and Windley (1984). Arc-accretion interpretations fail to explain the absence of high-P blueschist or eclogite facies rocks in or near the granite-greenstone terrains as expected in subduction settings, or crustal-scale Archean thrust zones (Rey and Houseman, 2006).

Other work supports a sagduction/diapirism interpretation for the Vermilion District (Sims, 1976; Hooper and Ojakangas, 1971), the Superior Province (Macgregor, 1951; Bedard et al., 2003; Lin, 2005) and other Archean provinces (Maufe et al., 1919; Macgregor, 1951; Anhaeusser et al., 1969; Mareschal and West, 1979; Collins and Van Kranendonk, 1998; Chardon et al., 2002; Rey et al., 2003; Van Kranendonk et al., 2004; Rey and Houseman, 2006). Results from modeling also suggest that formation of granite-greenstone terrains by sagduction and diapirism is plausible (Ramberg, 1981; Rey and Houseman, 2006). Data that supports the sagduction/diapirism hypothesis includes: 1) a consistent greenstone-down/granitoid body-up sense of shear in granitoid-body margins, 2) Fm and Le orientations that mimic granitoid boundaries, 3) low-grade metamorphic facies, 4) syn-doming features that conform with structural tests for diapirs and differ from those expected for metamorphic core complexes (Anhaeusser et al, 1969).

Anhaeusser et al. (1969) also asserted that a steeply plunging Le in volcanic rocks is characteristic of "all Precambrian greenstone belts." The presence of low-grade metamorphic assemblages and the absence of blueschist and eclogite facies in greenstone belts preclude the deep burial expected if these rock packages represented part of the root zones of orogenic belts (Burke and Kidd, 1978; Anhaeusser et al., 1969). Bedard (2003) suggests that the Minto Block of the northern Superior Province was not an accretionary orogen (as previously interpreted by Percival and Skulski, 2000), but rather, the result of sagduction/diapirism processes. Bedard (2003) cites the lack of terrane boundaries, the lack of structural repetitions in so-called 'accretionary' sequences, and finally, misinterpretations of phenomena that both hypotheses predict.

Certain lines of evidence are null with regard to either hypothesis depending on the scale or context of the observed data (Table 1). According to Harland's (1971) definition, transpression is obliquely convergent motion between two crustal blocks, or motion partitioned into convergence and strike-slip displacement. Although transpression can occur at a regional scale between two tectonic plates, transpression can also occur at the intragranular scale within a rock, as well as all intermediate scales (Robin and Cruden, 1994). Thus, transpression could occur both in arc-accretion and sagduction and diapirism. Therefore, evidence of transpression does not favor one hypothesis over the other (Table 1). Likewise, Anhaeusser et al. (1969) interpreted flattening parallel to schistosity as the result of contraction caused by granitoid emplacement. Craton-scale contraction (or oblique contraction, as is a common interpretation of the Superior Province) need not be invoked to explain the structures of typical greenstone belts; rather, regional contraction associated with granitoid bodies

could produce the flattening parallel to schistosity common in greenstone belts. Shallow Fm and dip-parallel Le in the Abitibi subprovince granite-greenstone terrain of the Superior Province characterize the thrusting event of arc-arc collision according to Mueller et al. (1996). However, these same structures could also form by sagduction and diapirism. Mueller et al. (1996) state, "local overturned mafic pillowed units suggest recumbent folding;" "en-echelon folds, shallow stretching lineations, and a late cleavage cross-cutting the folds support a dextral shear sense in [one segment] of the [fault zone study area]." Again, folded pillow lavas and local structures, if interpreted without domain trends, are not unique to either hypothesis. Craton-scale Archean strike-slip faults are ubiquitous in many Archean cratons such as the Superior Province, the Yilgarn craton of Australia, the Dharwar craton of India, or the Karilian craton of Russia. Various authors interpret strike-slip or transcurrent displacement as evidence of a post-thrusting arc fragmentation phase under regional oblique convergence and subduction (Mueller et al., 1996; Konopasek et al., 2004), yet Sims (1976) and Rey and Houseman (2006) assert that the convergence of warm and buoyant granitoid lithosphere would result in an overall transcurrent tectonic regime with strike-slip faults and crustal-scale gravitational flow controlled by high Archean heat flow. Crustal-scale Archean thrust faults appear absent and have yet to be documented in Archean cratons (Rey and Houseman, 2006). Rey and Houseman (2006) assert that the high Archean geotherm and a buoyant sub-continental lithospheric mantle would have impeded crustal thickening and promoted deformation over large areas through gravitational flow and strike-slip faults perpendicular to the direction of convergence.

The history of interpretations of granite-greenstone terrains, particularly different interpretations of the same data, reflects the nature of the on-going, and unsolved debate. Clearly there is room for new data, which might help to resolve the debate.

2.5 Study Region: KSZ

Granite-greenstone terrains commonly preserve shear zones, which may record a portion of the history of Archean crustal evolution and tectonic processes. This structural and kinematic analysis of the KSZ within the Vermilion District of the Wawa Subprovince, Superior Province, was conducted to determine the structural and kinematic history of the KSZ, and to examine how that history constrains tectonic evolutionary processes of the Vermilion district granite-greenstone terrain.

The KSZ is one of several east-northeast-striking, steeply-dipping shear zones in the Vermilion District of northeastern Minnesota (Fig. 2). The Vermilion *greenstone belt* (Fig. 5) comprises a package of greenstone, iron formation, metavolcanic and metasedimentary rocks bounded to the north by the Vermilion Granitic Complex (2.7 ± 0.052 Ga) and to the south by the Giants Range granitoid (2.67 ± 0.024 Ga) (Jahn and Murthy, 1975). Stratigraphically, mafic volcanic rocks comprise the Ely Greenstone, with upper and lower members separated by the Soudan Iron Formation. Mainly felsic volcaniclastic rocks and sedimentary rocks of greywacke affinity comprising the Knife Lake Group in the central part of the district and the Lake Vermilion Formation in the western part of the district overlie Ely Greenstone stratigraphically. Younger, mainly mafic volcanic rocks of the Newton Lake Formation overly the Knife Lake group and Lake Vermilion Formation (Sims, 1976 and references therein; Schulz, 1980).

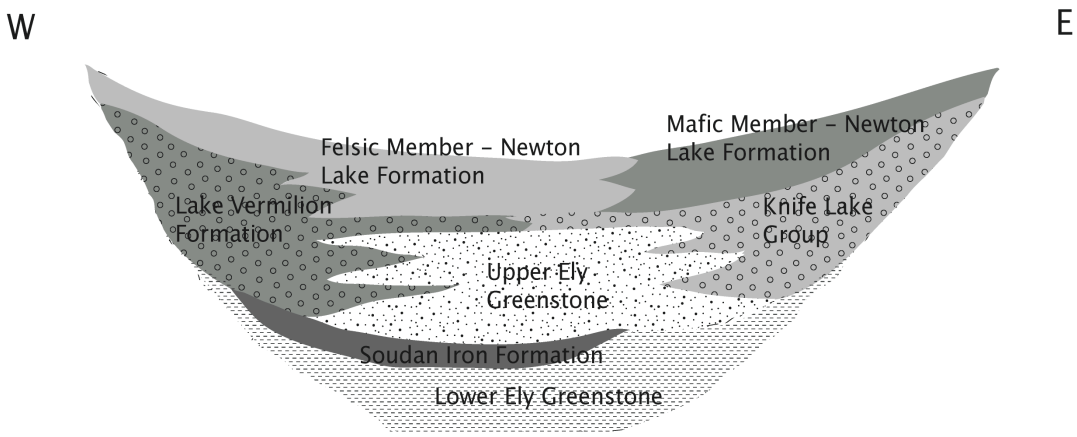

Figure 5. Vermilion greenstone belt cross-section cartoon shows reconstructed stratigraphic relationships, pre-folding and faulting (After Schulz, 1980).

The Vermilion Granitic Complex and Giants Range granitoid broadly bound the KSZ to the north and south, respectively. The ca. 30 km long KSZ is truncated by 1.1 Ga Keeweenawan intrusive rocks in the southeast and the north-striking Waasa fault in the west. Locally, the KSZ lies within Ely Greenstone (2.7 Ga); Knife Lake Group graywackes, tuffs, and conglomerates; and the Giants Range Batholith to the south and eastern extent (Fig. 2, Plate 1 a, b).

Various authors have investigated the structural history of the Wawa subprovince in general (Card, 1990) and much of the western Vermilion District (Hooper and Ojakangas, 1971: Bauer and Bidwell, 1990; Tabor and Hudleston, 1990; Jirsa et al., 1992). However, the structural history of the southeastern Vermilion District North Kawishiwi region has only been addressed as part of geologic work with a larger and more general scope (Green, 1970; Green et al., 1966; Sims, 1976).

Green (1970) and Green et al. (1966) provide a comprehensive summary of the bedrock geology and the structural history of the Kawishiwi Region. The bedrock geology along the North Kawishiwi River consists of the Knife Lake group: a thick group

of metaconglomerates and metagraywackes, now gneisses and schists, faulted against the lower part of the Ely Greenstone (Green, 1970) (Plate 1). A variety of porphyries, including a regionally widespread ~2.7 Ga porphyritic dacite-rhyodacite porphyry, intrude the stratified rocks. The Giants Range granitoid, dominated in the Kawishiwi region by a mostly non-porphyritic facies (gmh) and a porphyritic facies (gap), intrudes the Ely Greenstone and Knife Lake metasedimentary rocks along the North Kawishiwi River. Most of the contacts within the granitoid are unchilled, and suggest physical mixing of viscous magmas.

Green (1970) attributed the deformation of the Archean rocks to the Algoman orogeny (2.6-2.5 Ga) but overall, did not consider the sequencing of Archean deformation events. His description below outlines his main observations and interpretations of the Kawishiwi region, and corresponds to the data from his work shown in Plate 1.

> "The entire structural deformation of the Lower Precambrian rocks in this area is attributable to the Algoman orogeny (2.6-2.5 Ga). The strata are nearly vertical, and depositional structures indicate tops are generally to the north, away from the North Kawishiwi fault. There is local internal isoclinal folding, however, in all the formations. Faults are of particular significance, and at least some followed intrusion of the batholith. Several east-ward to northeastward-trending faults of regional importance cross the area, and lesser north-northeastward- and northeastward-trending faults with apparent displacements with as much as two miles cut the Ely Greenstone into many blocks. Strong, steeply-plunging lineations are widespread in the northern edge of the area and along the North Kawishiwi River. Kink-folds with gently-plunging or vertical axes, which represent minor displacements and a higher level of deformation, are superimposed on the earlier structures, especially in a zone centered in the Knife Lake belt. Their age is unknown but is probably late Algoman.
>
> Metamorphism of the stratified rocks is generally of very low grade (greenschist facies), and a lack of equilibrium is widespread. Near the Vermilion and Giants Range batholiths, epidote-amphibolite and amphibolite facies are attained, and next to the Duluth Complex [1.1 Ga Keeweenawan Intrusions] is a narrow zone of pyroxene hornfels."

This structural and kinematic investigation focuses on the kinematic history recorded by the widespread steeply-plunging lineations [confirmed by Green as Le (pers. comm, 2007)] that Green (1970) observed, as well as the zone regarded as the Kawishiwi Fault where Le are generally horizontal.

Sims (1976) interpreted the Kawishiwi region with respect to the broader Vermilion District, and proposed a sequence of Archean deformation events strongly related to rising granitoid bodies. He contended that the volcanic-sedimentary belt folded contemporaneously with emplacement of the Vermilion Batholith (granitoid body) and Giants Range granitoid body. The relative upwelling and convergence of the buoyant granitic bodies produced a compressive stress and led to shortening and folding. Metamorphism of the supracrustal rocks to greenschist and, locally, middle-amphibolite facies, accompanied the folding. Later, anorogenic monzonite rocks intruded the supracrustal rocks as diapirs. Three steep fault sets postdate Vermilion District folding: 1) vertical dip-slip faults, 2) dextral strike-slip faults, and 3) transverse (northeast-trending) left-lateral strike-slip faults (Sims, 1976). Regional strike-slip faulting followed emplacement of the anorogenic plutons. The Kawishiwi Fault is part of the Vermilion Fault system, consisting of the Vermilion Fault in the west and splays into the Burntside Lake Fault and the Wolf Lake to North Kawishiwi Fault in the east (Sims, 1976). These steep faults are marked by what Sims (1976) calls ≤150 m-wide "cataclasite" zones. Cataclasite was previously used to describe what is now known as a *ductile* 'mylonite' texture; 'cataclasite' is now reserved for *brittle* deformation textures. It is unclear if Sims meant 'mylonite' to indicate brittle or ductile deformation. The faults typically follow topographic depression, a common result of eroded brittle cataclastic zones, and/or linear

waterways. Sims (1976) suggested dextral strike-slip offset could be 17 to 19 km along the fault system. He interprets the following as offset markers along the Kawishiwi fault: 1) the central KSZ and Snowbank Lake granitoid bodies and 2) the Knife Lake group east of White Iron Lake and the Knife Lake group north of Lake One (Plate 1). Sims concludes that the strike-slip faulting marked the transition from an unstable crust dominated by vertical tectonic movements to a more stable crust capable of sustaining regional fractures. The observations and interpretations of Green et al. (1966), Green (1970) and Sims (1976) provide both broad framework data and ideas from which this re-evaluation of the KSZ continues.

This re-evaluation of the KSZ structural and kinematic history relies on the information of the structural fabrics: foliations, lineations, and petrofabrics.

2.6 Structural Fabrics: Definitions and Utility

Planar features that occur penetratively in a body of rock, excluding joints or bedding, are foliations (Fig. 6 and Table 2). Metamorphic foliations (Fm) are secondary foliations typically defined by: 1) compositional layering, 2) preferred orientation of platy minerals (e.g. mica), 3) preferred orientation of grain boundaries and the shape of recrystallized grains (e.g. quartz, carbonate) in a grain shape preferred orientation, or 4) preferred orientation of platy minerals in a matrix without preferred orientation (e.g. mica in micaceous quartzite or gneiss) (Fig. 6 and Table 2). Fm generally form parallel to the plane of flattening of the finite strain ellipsoid (Twiss and Moores, 1992). Strike (azimuth) and dip (angle from horizontal) of the plane quantifies the Fm orientation.

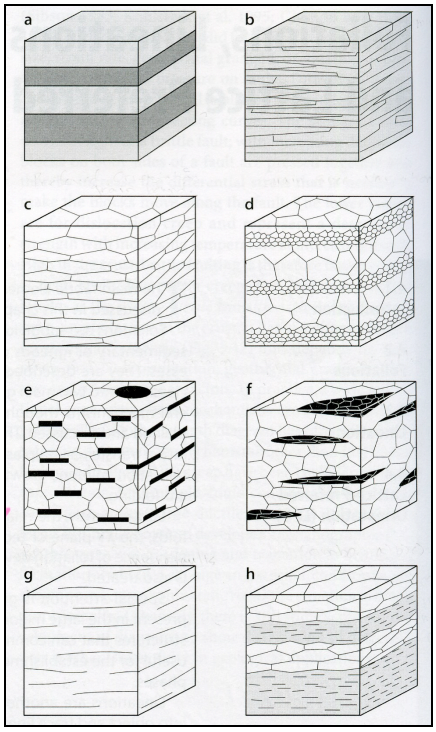

(from Passchier and Trouw, 2005)

Figure 6. Fabric elements that may define a foliation include: a) compositional layering, b) preferred orientation of platy minerals (e.g. mica), c) preferred orientation of grain boundaries and shape of recrystallized grains (e.g. quartz, carbonate) in a grain shape preferred orientation, d) grain-size variation, e) preferred orientation of platy minerals in a matrix without preferred orientation (e.g. mica in micaceous quartzite or gneiss), f) preferred orientation of lenticular mineral aggregates, g) preferred orientation of fractures or microfaults (e.g. in low-grade quartzites), and h) a combination of fabric elements a, b and c; such combinations are common in metamorphic rocks

Table 2. Criteria to distinguish primary and secondary foliations

Primary Foliation	**Secondary Foliation**
Sedimentary structures present	No sedimentary structures present
Thickness of layers may show any variation, especially across strike	Little variation in thickness
Variable composition and grain size	Composition of layers usually bimodal
Planar layering	Layering commonly lensoid or anastamosing
Rarely a symmetry plane parallel to layering	A symmetry plane parallel to layering common
Foliation never parallel to the axial plane of folds	Foliation (sub)parallel to the axial plane of folds of an earlier foliation

(from Passchier and Trouw, 2005)

Linear features that occur penetratively in a body of rock are lineations (Fig. 7). Lineation trend (azimuth) and plunge (angle from horizontal) in space or a pitch angle of the lineation within a plane quantify a lineation orientation. Pitch quantifies a lineation orientation as an angle from the horizontal strike of the foliation plane. Pitch represents lineation within the foliation plane. Elongation or stretching lineations (Le), one type of object lineations, form by preferred orientation of elongate mono- or polycrystalline objects whereby, aggregates commonly lie in the direction of maximum stretching, the X-axis of the finite strain ellipsoid (Twiss and Moores, 1992)(Figs. 7 and 8). The X-axis indicates the direction of tectonic transport if Le form in ductile shear zones with approximately simple shear flow (Passchier and Trouw, 2005) (Fig. 8, stretching lineation). However, Le also form normal to the displacement direction (Passchier, 1998; Sengupta and Ghosh, 2004) (Fig. 8, rolling lineation). Kinematic vorticity, preserved by some naturally deformed rocks, measures the rotational flow type and non-coaxiality (Passchier and Trouw, 2005; Tikoff and Fossen, 1995). To determine shear sense, one must determine the vorticity axis orientation with respect to the Le orientation (Fig. 8). This determination is critical to the structural and kinematic history of the KSZ.

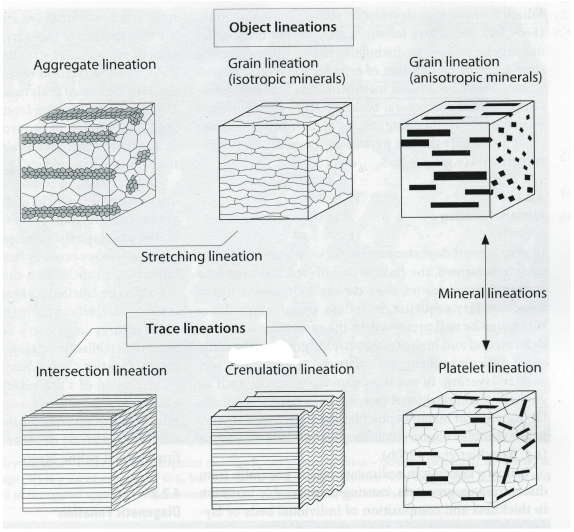

Figure 7. Cartoon shows fabric elements that may define a lineation. (from Passchier and Trouw, 2005)

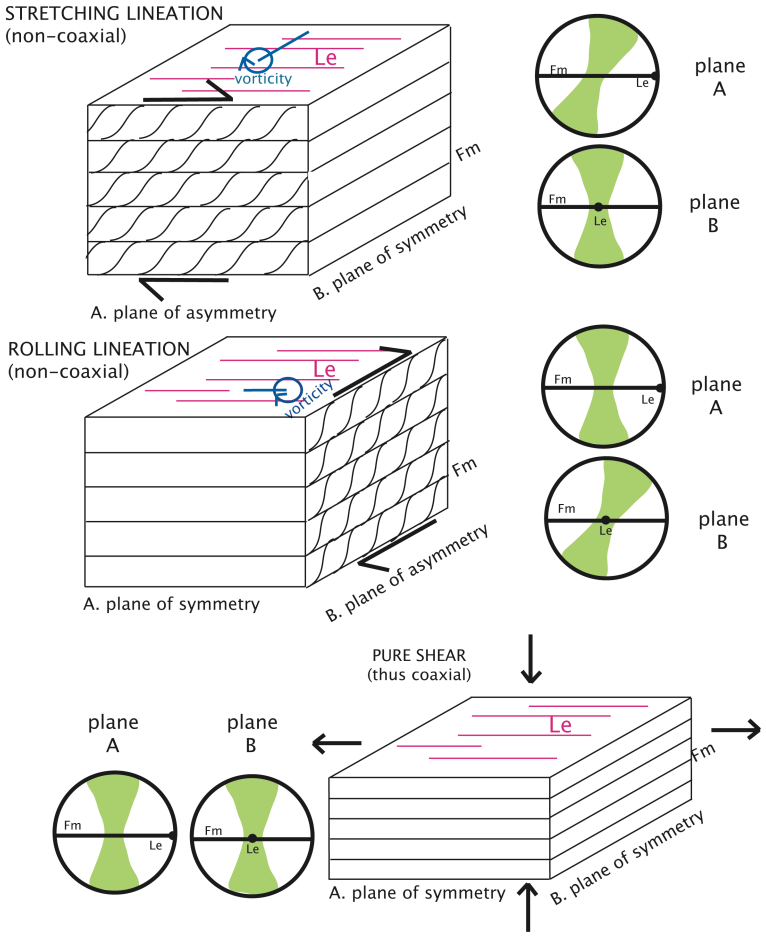

Figure 8. Cartoon of relationship of Le to: Fm, planes of a/symmetry, vorticity, and quartz c-axis girdles.

Mineral lattice preferred orientation (LPO) diagrams can provide clues about the operative slip systems during tectonic deformation. Slip systems, crystallographic axes, and fabric elements tend to rotate towards the fabric attractor, resulting in a common orientation of components of the LPO and reference Fm and Le (Fig. 8). LPO forms easily in micas or amphiboles as a foliation or lineation because mica and amphibole crystals are planar or elongate, respectively. For quartz, a-axes and c-axes record the LPO; these then indicate the orientation of the various slip planes. Quartz occurs not only in granitoid rocks but also in metasedimentary and metavolcanic rocks in the KSZ volcano-sedimentary package. The U-stage method determines quartz c-axis LPO and its slip plane. Quartz c-axis LPO increases in strength and sharpness with increasing strain, and undergoes only slight changes in geometry (Passchier and Trouw, 2005). LPO asymmetry reflects vorticity. In initially isotropic materials, non-coaxial progressive deformation leads to LPO patterns with monoclinic symmetry (one mirror plane in 3-D) whereas, co-axial progressive deformation leads to patterns with higher symmetry (three or more planes) (Passchier and Trouw, 2005). Thus, a comparison of Le orientation to LPO diagrams allows assessment of whether Le formed normal or parallel to displacement direction (Fig. 10). Quartz c-axis LPO patterns also record metamorphic grade because activation of quartz slip-systems depends, in part, on temperature (Fig. 9).

In the case of non-coaxial progressive plane strain deformation (simple shear) of quartz, asymmetric Type-I crossed girdles, and single girdles inclined to Fm and Le are common (Passchier and Trouw, 2005). At medium to high-grade metamorphic facies, single maxima around the Y-axis are common, whereas at high-grade (>650°C), point maxima in a direction close to Le occur (Passchier and Trouw and references therein,

2005). At conditions below 650°C, slip in <a> directions on basal, prism and rhomb planes dominates. At low temperature (< 350°C), basal <a> slip is most important and the girdles have a strong cluster of c-axes in the periphery. With increasing temperature, prism <a> slip becomes more important and the girdle tends to a maximum around the Y-axis. At very high temperature (> 650°C) and hydrous conditions (i.e. granulite facies), prism <c> slip operates, and causes a c-axis maximum sub-parallel to the attractor, and <a> axes normal to it (Fig. 9).

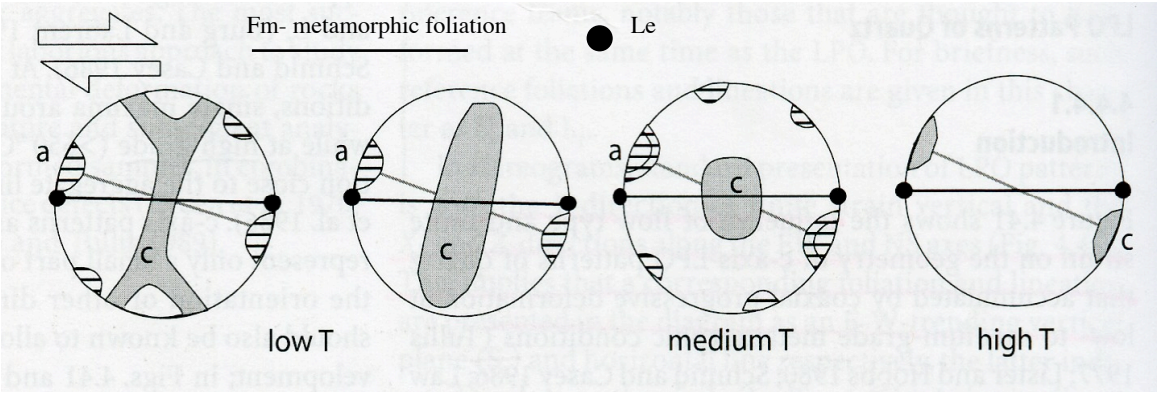

Figure 9. Lower hemisphere, equal area pole diagrams showing four types of contoured LPO patterns of quartz c-axes (*grey*) and a-axes (*striped*) that develop with increasing metamorphic grade in non-coaxial progressive deformation. The variation is due to a change in the dominant slip systems. (from Passchier and Trouw, 2005)

Rock mineral assemblages, fabric elements, and deformation types are important for this study. Rock mineral assemblages indicate metamorphic facies, which reflect pressure-temperature (P-T) conditions or the crossing of a reaction equilibrium curve in P-T space. In addition, quartz, calcite, feldspars, micas, olivine, orthopyroxene, clinopyroxene, garnet and amphiboles have predictable grain-scale deformation at certain grades of metamorphism, providing further clues of metamorphic facies conditions that accompanied deformation (Appendix, Table 1). Ductile deformation occurs at higher

metamorphic grade and lower strain rate, resulting in mylonites, foliated and lineated rocks (L-S tectonites) with characteristic porphyroclasts in a finer-grained matrix. Brittle fabrics include gouge, breccia, cataclasite and cataclastic flow. The sagduction/diapirism hypothesis predicts solid-state granitoid deformation with partial melting possible. Magmatic structures and fabrics in granitoid bodies reflect pluton or diapir emplacement and processes such as replenishment, convection, mixing, crystallization, deposition and compaction that operated in an active magma chamber during solidification or, possibly to a lesser degree, during diapir emplacement (Wiebe and Collins, 1998; Passchier and Trouw, 2005).

This study reports KSZ structural and kinematic elements including: 1) metamorphic facies, 2) Fm, 3) Le, 4) LPO and quartz c-axis orientations, 5) metamorphic facies and 6) shear sense indicators.

3. Methods

The objective of this study was to determine the structural and kinematic history of the KSZ. The kinematic and structural methods include: 1) compilation of structural and bedrock geology data in a GIS; 2) new fieldwork to collect oriented samples, and additional structural data including: Fm, Le, and kinematic indicators; 3) petrography to identify mineral assemblages; 4) microstructural kinematic analysis of oriented thin sections; and 5) universal-stage petrofabric analysis of quartz c-axes.

3.1 GIS: Compilation of Existing and New Data

Different parties have mapped the KSZ field area. The bedrock geology, Fm, Le, and bedding data were particularly useful as a fieldwork guide as well as to provide data for areas where new fieldwork data was not collected (Fig. 10). Bedrock geology from Minnesota Geological Survey (MNGS) maps M-148 (Jirsa and Miller, 2004) and digitized structural data (Green et al., 1966; Green and Shulz <sic>, 1982) were compiled in ArcView 9.2™. The final shapefiles (appendix c.d.) include MNGS maps: 1) 1:100,000 Bedrock Geology of the Ely and Basswood Quadrangles, NE Minnesota shapefiles (Jirsa and Miller, 2004) for a bedrock geology base map, and 2) geo-referenced images (geotiffs) of the 1:31,680 Geologic Map of Gabbro Lake Quadrangle (Green et al., 1966), and 3) the 1:24,000 Geologic Map of Ely Quadrangle (Green and Shulz, 1982). Orientations of bedding, Fm and Le were digitized from the Gabbro and Ely quadrangles for data analysis.

New data from fieldwork (Fm, Le, bedding, sample locations, thin section index, and lithology) were compiled in a shapefile (*SG_fielddata* in appendix, c.d.). Where multiple data measurements are recorded for a single outcrop or small area, data are reduced to an average plane or line (determined by stereonet) for map Plate 1. Multiple measurements are shown (not averaged) if they had a significant (≥ 25° strike or trend, ≥ 15° dip or plunge) difference in orientation. New field data remains in shapefile *SG_fielddata*. Simplified new field data for the final map is in shapefile *Abbrev_S.G.fielddata*. The structural data from the Gabbro Lake and Ely quadrangles is distinguished from my own fieldwork data in the GIS attribute tables (shapefile

Sal_Gabbro1966_Ely1982), and thus data separation and comparisons are easily facilitated.

The compiled existing and new data are used to create Fm trajectory (lines), pitch domain (polygons), general geology (polygons), and sample location, kinematic confidence layers and shapefiles. Final map plate layouts were assembled in Adobe Illustrator™(Plate 1).

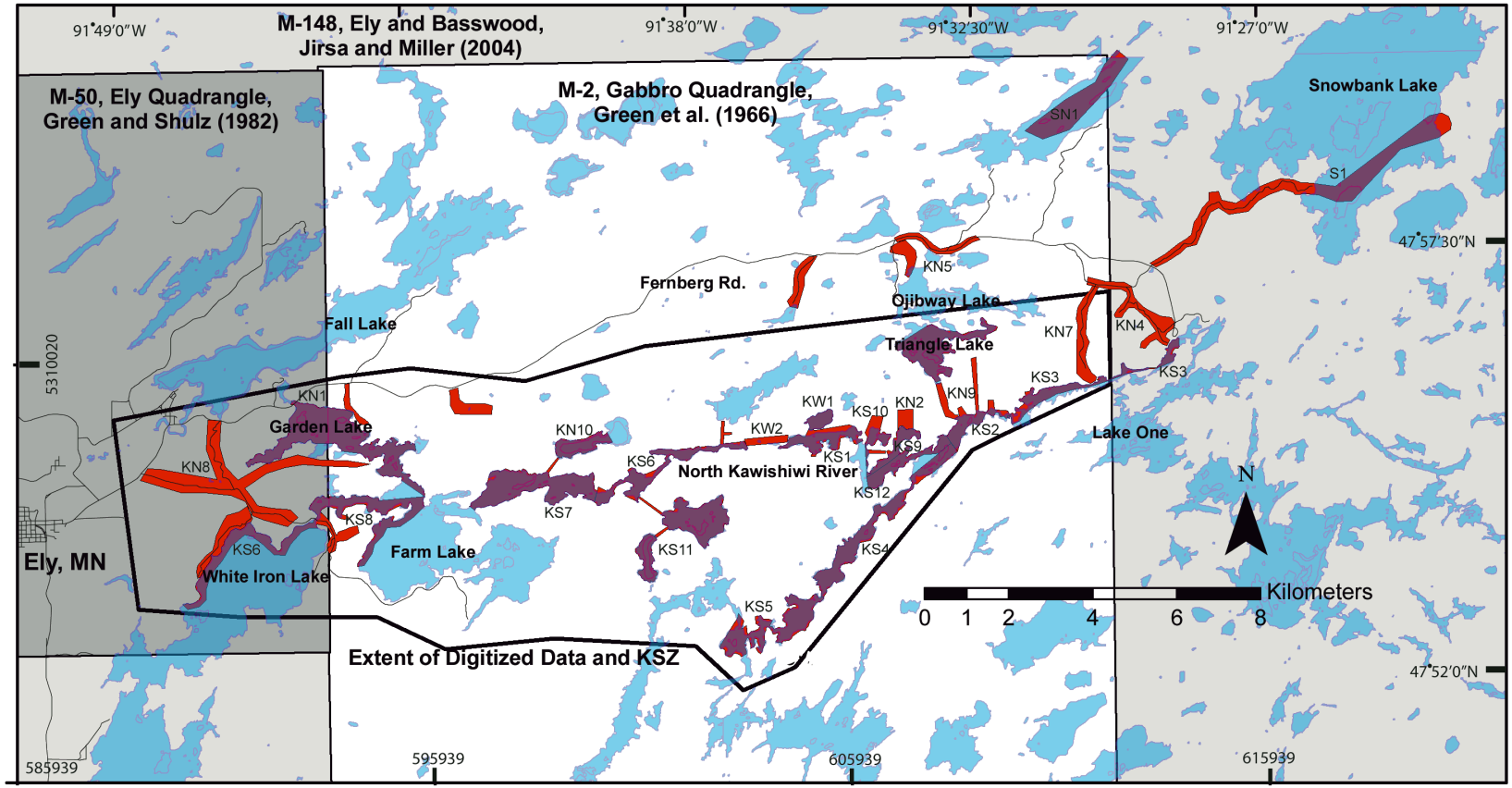

Figure 10. This map shows the data sources and areas for digitized map data. The red and purple areas are the zones studied in this research. Zone notations (KS1, KN1, etc.) coorespond with sample and thin section notations. Purple areas mark north-south and east-west transects and waterline outcrops accesed by canoe. Red areas mark land investigated on foot.

3.2 Fieldwork

Fieldwork involved collecting oriented samples (Hansen, 1990) noting locations (latitude and longitude with GPS) and orientations of general lithologies, Fm and bedding planes, Le, kinematic indicators, and minor folds. Field mapping focused along the ca. 24 km E-W strike of the KSZ and in ca. 8-10 km N-S transects across the KSZ. Most of the KSZ lies within the Boundary Waters Canoe Area Wilderness (BWCAW), with travel limited to canoe, foot/ski/snowshoe, or dogteam. In order to cross from predominantly greenstone to the north to the Giants Range granitoid to the south, KSZ transects follow portages and waterways (Fig. 10).

Structural data indicate the extent and character of structural domains across and within the KSZ. Foliation is classified as bedding, igneous layering (primary foliations), or as Fm. Fm includes secondary foliations of mylonitic foliation, preferred orientation of grain boundaries and shape of recrystalized grains, schistosity and bedding parallel compositional layering (Fig. 6 and Table 2). Le are the most prevalent type of lineation.

The re-evaluation and further elucidation of structural elements from published maps was valuable on several levels. Fieldwork largely served as confirmation of mapping accuracy and thus, data utility for this study, although the nature of some of the foliations, lineations, or lithologies is locally reinterpreted. Previous studies did not consider microstructural kinematic shear sense indicators and petrofabric development (a field of investigation that emerged after these early works), which requires oriented samples from a geographic distribution of locations, such as along transects.

3.2.1 Justification for Changes to Existing Maps of KSZ

My interpretations of KSZ rocks dictated some methodology changes as fieldwork progressed. As noted, magmatic foliation could occur in pluton or diapir emplacement. In Giants Range granitoid rocks, the distinction between a primary magmatic foliation and a secondary Fm, commonly defined by the orientation of amphibole, was indistinguishable in the field. Therefore, after the first round of fieldwork in the BWCAW extending 7 km south of the *Kawishiwi Fault* (so-mapped by Green et al., 1966) on the South Kawishiwi River where the nature of the foliation was indistinct, I focused on granite and orthogneiss (gneiss of igneous origin) within three km of the Kawishiwi Fault where amphibole defined a pronounced Le within moderately developed Fm planes.

Shear plane symbols of the Gabbro (1966) and Ely (1982) quadrangles represent different types of planar phenomena. On the Gabbro Lake Quadrangle, the markings represent discrete (≤ 1m wide) shear zones commonly within granitoid rocks (Fig. 11). The attitude of these shear zones is indeterminate, due to the smooth granitoid outcrop surfaces that disallowed a 3-D view of the structure; these locations remain as mapped by Green et al. (1966) in the GIS digitized points.

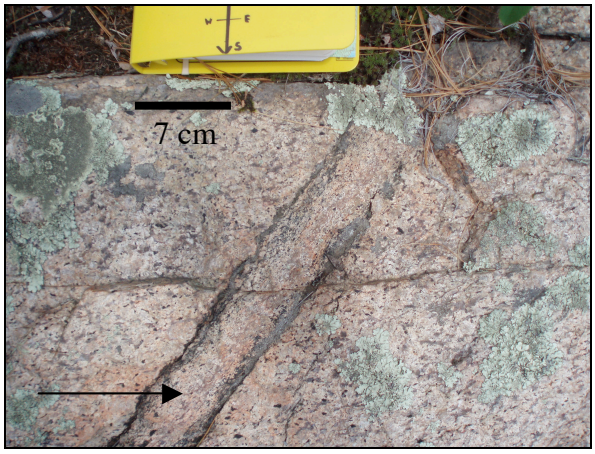

KS5B: N47° 52.932', W091° 36.222'

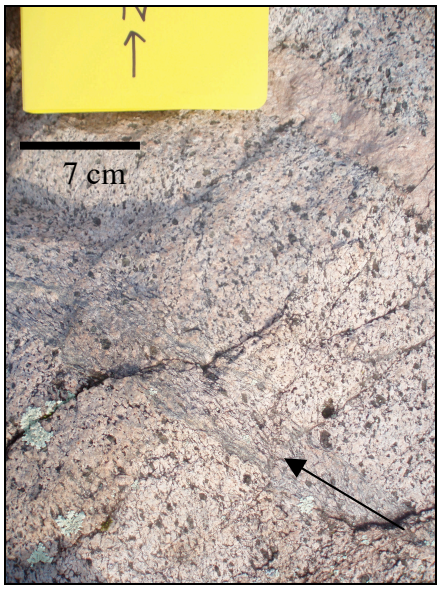

KS3B: N47° 55.521', W091° 31.526'

Figure 11. Photographs of discrete shear planes (indicated by arrows) from locations KS5B and KS3B. Discrete shear planes are the cm-wide zones surrounded by massive granite.

KS9K: N47° 55.242', W091° 33.860'

Figure 12. Field photograph of foliated and lineated orthogneiss from location KS9K. The zone shown here contains both Fm and Le and is continuous across a several-meters-wide shear zone. The view direction is Fm-perpendicular and Le-parallel (Le not visible in the plane shown).

I interpreted the other shear plane markings as planar Fm (Fig. 12). They commonly occur in a 500 m-wide zone along the Kawishiwi Fault (as defined in the Gabbro Lake quadrangle, 1966). The final map shows Fm symbols in place of shear plane symbols in those locations (Plate 1). Shear planes on the Ely Quadrangle (1982), described as "late shear surfaces" mark slickenside planes; slickenside striations, surface lineations, as opposed to Le, do not penetrate the rock. I give the slickenside-containing planes a new symbol on the final map (Plate 1). Original shear plane locations can be viewed in the GIS shapefile geotiff map image layers (Appendix, c.d.).

Green et al. (1966) classified the bedrock between the Ely Greenstone and Giants Range granitoid body as Knife Lake Group (map unit *kg*). However, Jirsa and Miller (2004) classified the same bedrock as upper Ely Greenstone calc-alkalic volcanic rocks (map unit *Aec*). Noting a strong Le throughout the unit, and a similarity in occurrence of Le as well as lithology to the Knife Lake Group exposed in the Moose Lake region, I maintain the classification of Green et al. (1966), as Knife Lake Group.

I evaluated Le and Fm data from fieldwork and published maps. Fieldwork and published data were used to make Fm trajectories, stereonet plots of bedding, Fm and Le, and a pitch map. A Fm trajectory line represents similar Fm orientations over an area. J. Green confirmed (pers. comm., 2007) that the lineations on the Ely and Gabbro quads are indeed Le. Pitch of Le was calculated from locations with Fm, shear planes, and bedding in combination with Le using structural data from new fieldwork and the Gabbro Lake and Ely Quadrangles. Within the KSZ region, compositional banding (bedding) parallels Fm, therefore the bedding planes paired with Le data in the Gabbro (1966) and Ely (1982) quadrangles are used in pitch calculations.

3.3 Laboratory Work: Petrography, Microstructure and Petrofabric Analysis

Oriented samples were cut into oriented chips for standard thin sections prepared by Vancouver Petrographics, BC. Thin sections were used to determine metamorphic grade, kinematic indicators from microstructures and quartz c-axis fabrics (LPO) using the universal-stage (U-stage) method.

3.3.1 Metamorphic Facies

Rock mineral assemblages, microstructure relationships, and quartz LPO record metamorphic facies (Appendix Tables 1, 2, 3 and Figures 10, 11, 15) (Passchier and Trouw, 2005; Winter, 2000). Changes in P-T conditions cause changes in mineral assemblages. Thus, mineral assemblages indicate P-T conditions, or metamorphic facies, and the geothermal gradient to which a rock was subjected.

3.3.2 Microstructure Analysis

Rock microstructures can include kinematic indicators. For this study microstructures revealed more kinematic indicators than field outcrops. Shear sense indicators can include ductile microstructures: displacement markers, mantled porphyroclasts, strain shadows and caps, mineral fish, S-C fabric, sigmoids, deformed veins, tension gash veins, asymmetric boudins, and fragmented porphyroclasts, and brittle microstructures: displacement markers, incohesive and cohesive brittle fault rocks, pseudotachylyte, and slickensides (Fig. 13) (Passchier and Trouw, 2005).

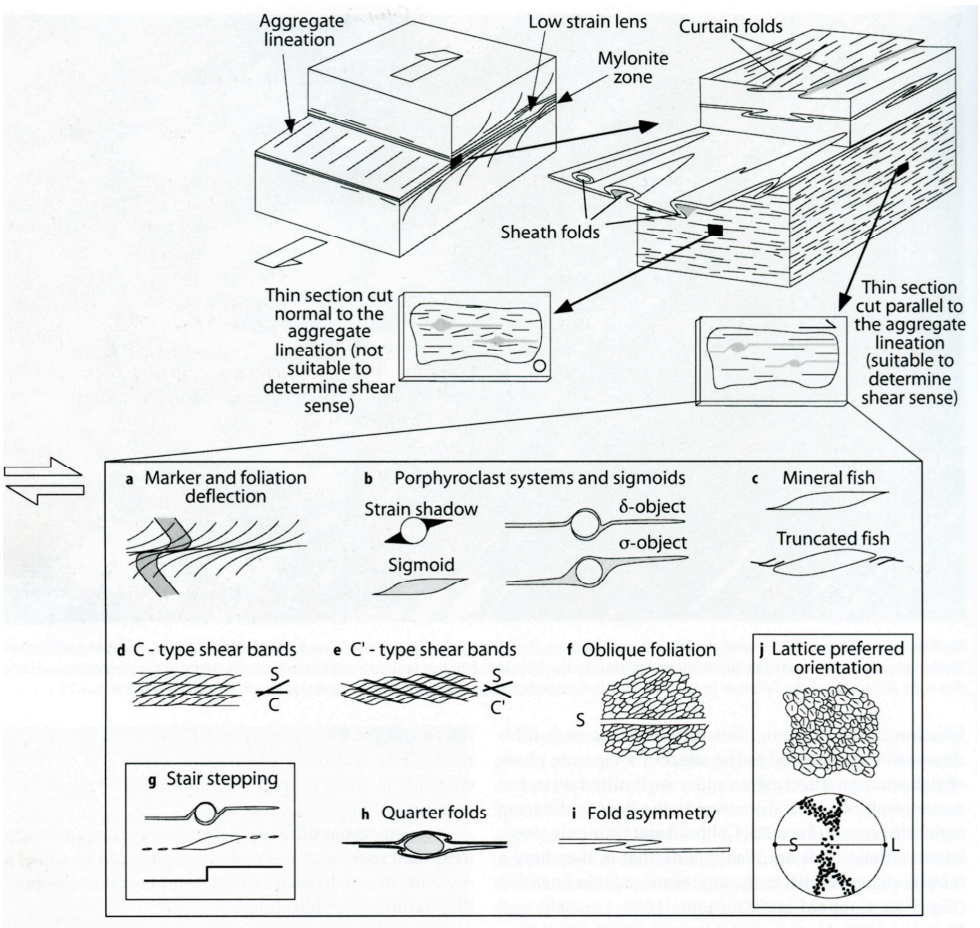

Figure 13. Geometries of a ductile shear zone or mylonite zone. For thin sections parallel to the aggregate lineation, the most common types of shear sense indicators are shown. (from Passchier and Trouw, 2005)

3.2.3 Petrofabric analysis: quartz c-axis LPO

Quartz c-axis LPO analysis provides a non-subjective record of strain history, shear sense, and clues to metamorphic temperature. However, it requires L-S tectonites with monomineralic quartz regions. A petrographic microscope fitted with a U-stage was used to measure the c-axis orientations of individual quartz grains relative to the sample and U-stage orientations (Turner and Weiss, 1963; Hallimond, 1970; Wahlstrom, 1979; Passchier and Trouw, 2005).

4. RESULTS

The results of this study, compiled within a geologic map include: 1) Fm trajectories, 2) pitch domains, and 3) ductile shear displacement. Results are considered with respect to time and multiple regional events.

4.1 Field Data

4.1.1 New and Existing Data

This study documents and utilizes both new and existing data (Plate 1). Lower hemisphere, equal area stereonets show: 1) bedding planes, 2) Fm planes, 3) Le (justification of classification as an elongation lineation, Le, in section 4.2.2) (Fig. 16 and Plate 1). Bedding orientations range within 360 degrees of strike and dips from 50° to vertical, with average bedding ~080, 75 N (Fig. 14, a and d). The average bedding and Fm planes are sub-parallel with average Fm ~075, 90 (Fig. 14, d). Le generally plunges steeply with a range of trend with average Le ~350, 85 (Fig. 14, c and d).

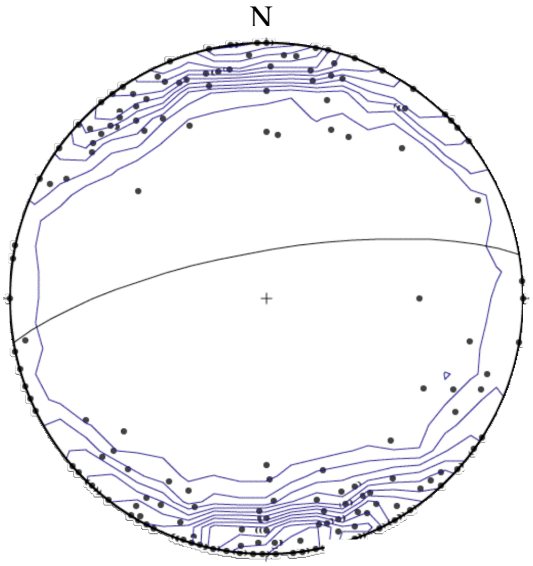

a) Poles to bedding planes and average plane
n=242, avg.: 260, 75 N
Kamb contours, contour interval = 2.0σ

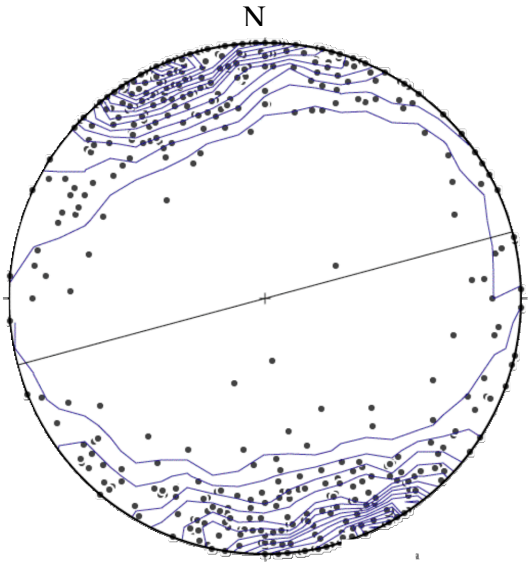

b) Poles to Fm planes and average plane
n=546, avg.: 255, 90 N
Kamb contours, contour interval = 2.0σ

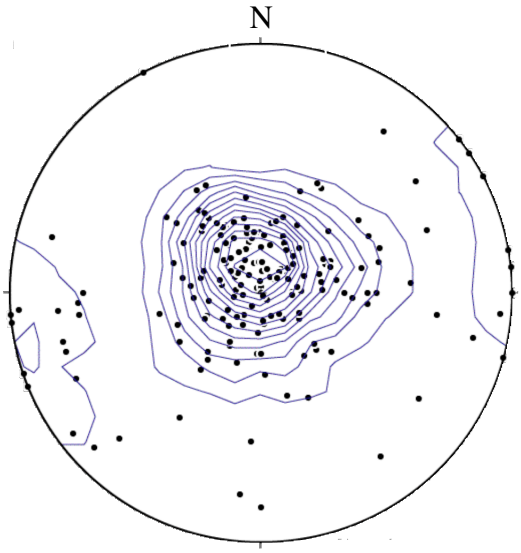

c) Le
n=199
Kamb contours, contour interval = 2.0σ

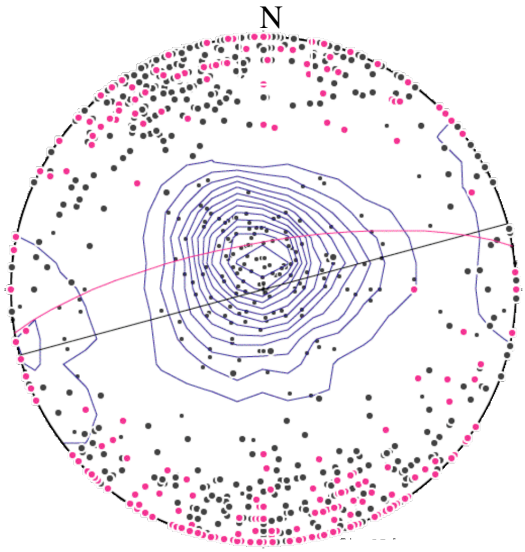

d) Poles to bedding (pink) and Fm (gray) with average planes, Le (small black dots) and Le Kamb contour interval = 2.0σ

Figure 14. Bedding, Fm, and Le equal area, lower hemisphere stereonets show data from this study, Green et al. (1966), and Green and Shulz (1982). a), b) and c) show data separately; d) shows bedding, Fm and Le data together. *Stereonet 6.3.3 X* used to plot and contour data. Contours show a 2σ statistical confidence interval.

4.1.2 Fm Trajectories

Fm trajectories within the KSZ, although regionally consistent, show local variations (Fig. 15). Consistently east-northeast oriented trajectories occur in the northern KSZ (north of the North Kawishiwi River), within the Ely Greenstone, and in the eastern KSZ within the Giants Range granitoid body. These consistent Fm trajectories parallel the strike of regional volcanic unit contacts. Varied and curvilinear Fm trajectories occur in the southwestern KSZ (south of the North Kawishiwi River) within the Knife Lake Group, some of the Ely Greenstone, and the Giants Range granitoid body. Curvilinear Fm trajectories within the Keeweenaw Intrusion rocks approximately parallel the contact between the 1.1 Ga intrusive rocks and the Archean rocks. It is unclear which present-day Fm in the Giants Range granitoid body and northeastern KSZ originated from the Keeweenaw intrusions, or, if the Archean Fm controlled the younger Keeweenaw-age Fm.

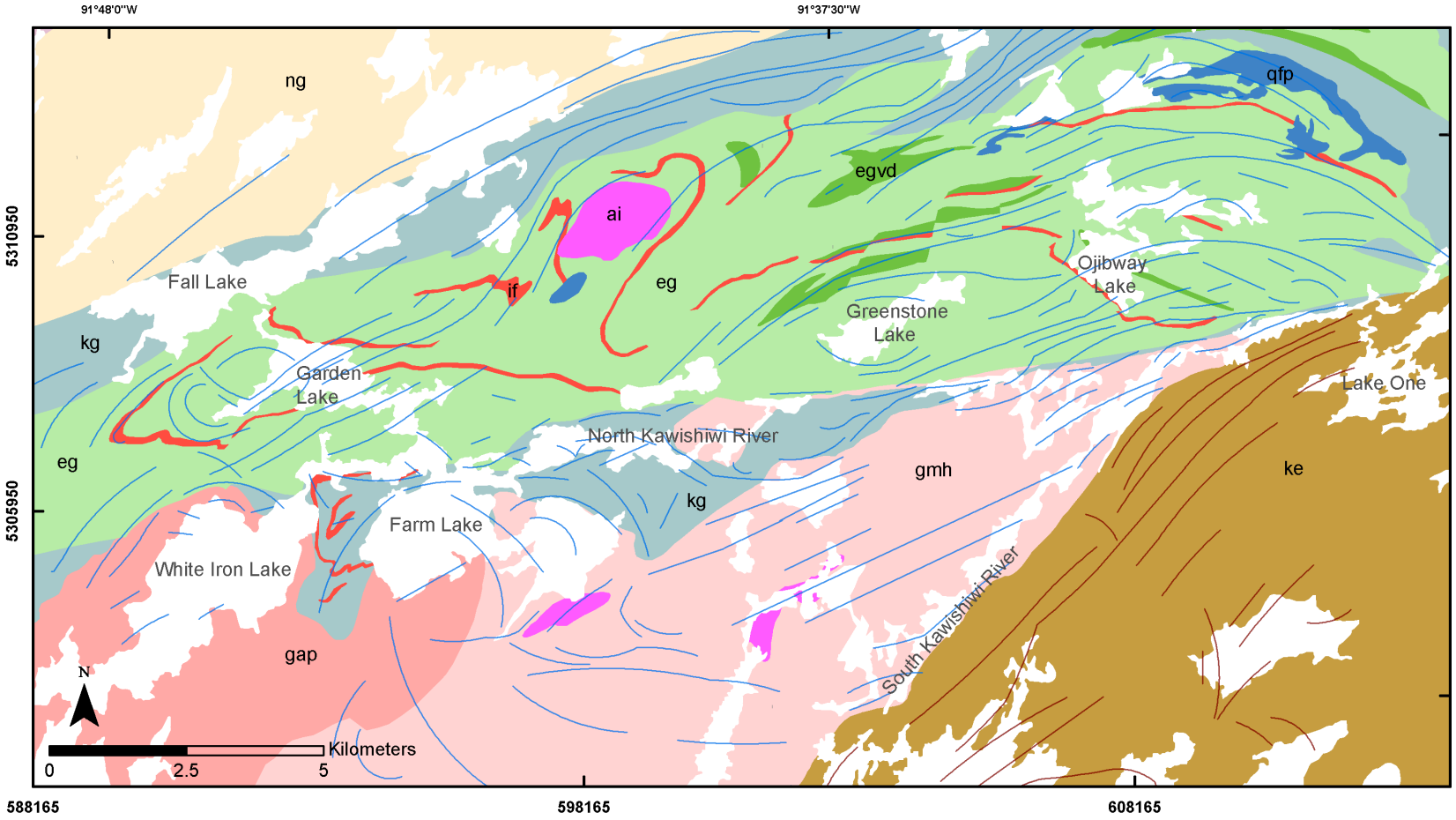

Figure 15. This map shows Fm trajectories within and surrounding the KSZ. Blue lines represent trajectories in Archean rocks, brown lines represent trajectories in Keeweenawan rocks. Bedrock units are: ke= 1.1 Ga Keeweenawan intrusion, gmh= Giants Range quartz monzonite and monzogranite, gap= Giants Range quartz monzonite, monzodiorite and monzogranite, ai= mafic and ultramafic intrusions, ng= Newton Lake metavolcanic and volcaniclastic rocks, qfp= quartzofeldspathic porphyry intrusions, kg= Knife Lake metavolcanic and clastic rocks, egvd= Ely verulitic greenstone and metadiabase, eg= Ely greenstone and greenschist, if= iron formation. White areas are lakes.

4.1.3 Pitch Data: Relationship of Fm and Le

Pitch values here represent the angle of Le from easterly Fm strike and therefore range from 0 to 180. Le within the KSZ fall into four domains with bimodal distribution: dominantly steep (50-130) and minor shallow values (0-30 and 150-180) and, there is a general lack of values from 30-50 and 130-150 (Fig. 16). In mapview, pitch domains show a distributed region of high pitch values and a narrow zone of low pitch values along strike of the KSZ (Fig.17).

a) Le pitch values

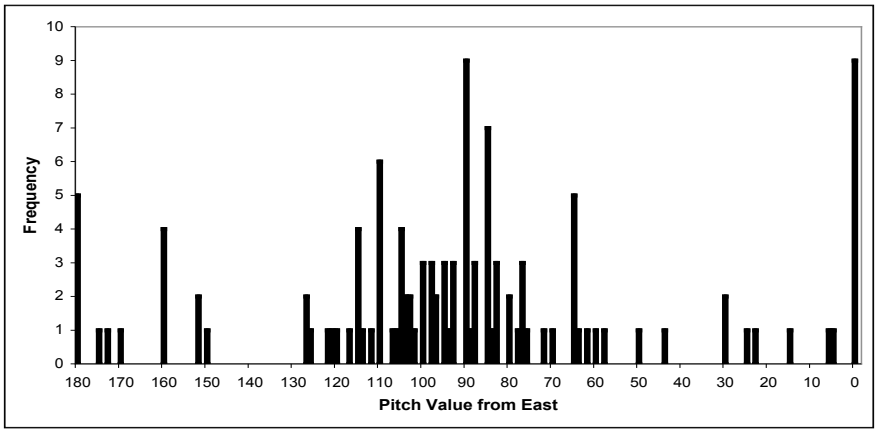

Data from S. Goodman, Green et al. (1966), and Green and Shulz (1982), n=120.

b) Pitch domain bins

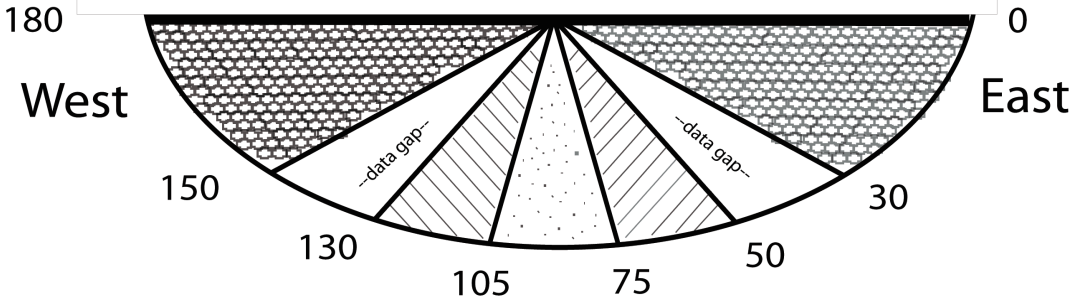

Figure 16. KSZ Le values shown as a) pitch and b) pitch domain bins.

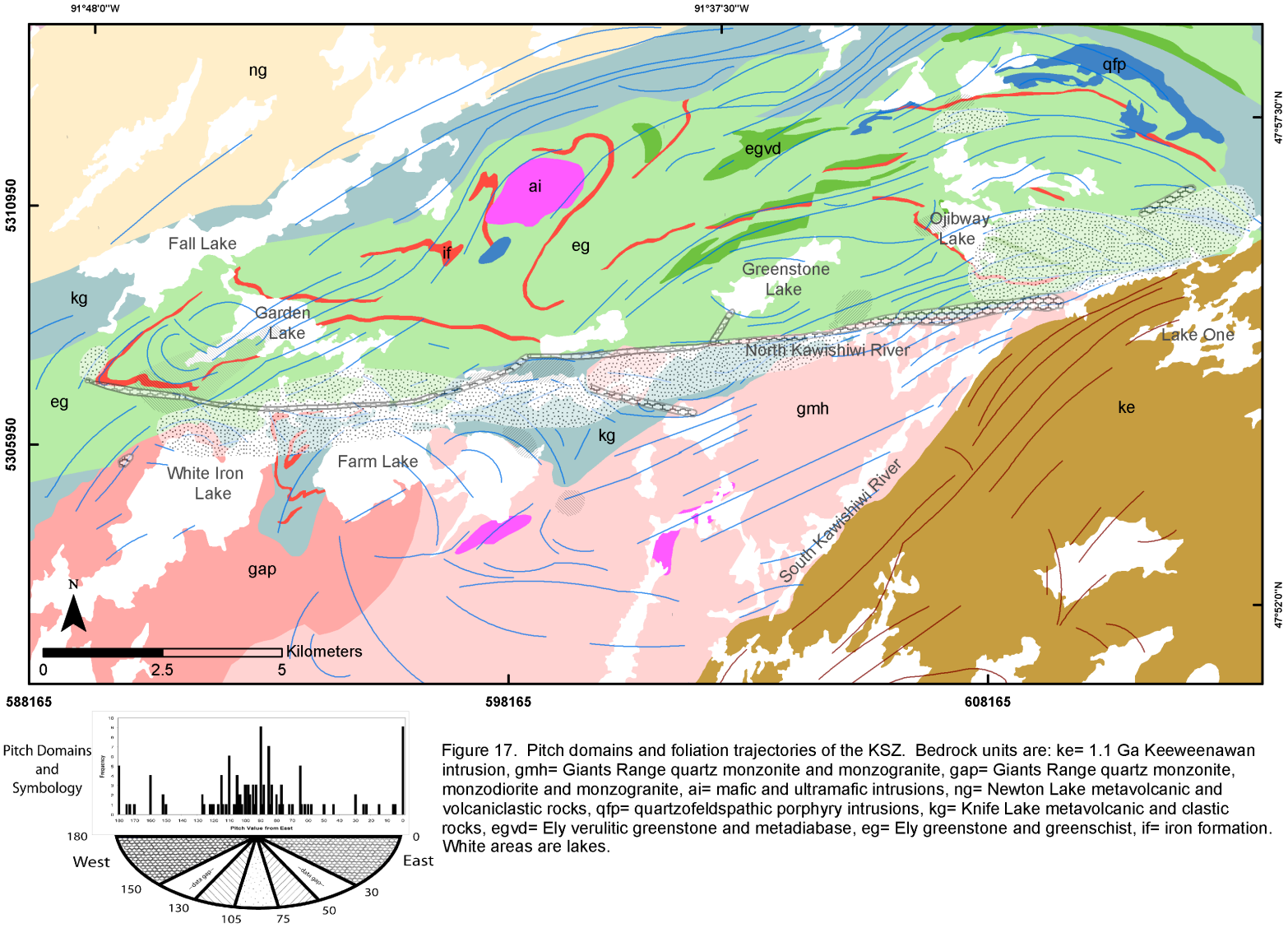

Figure 17. Pitch domains and foliation trajectories of the KSZ. Bedrock units are: ke= 1.1 Ga Keeweenawan intrusion, gmh= Giants Range quartz monzonite and monzogranite, gap= Giants Range quartz monzonite, monzodiorite and monzogranite, ai= mafic and ultramafic intrusions, ng= Newton Lake metavolcanic and volcaniclastic rocks, qfp= quartzofeldspathic porphyry intrusions, kg= Knife Lake metavolcanic and clastic rocks, egvd= Ely verulitic greenstone and metadiabase, eg= Ely greenstone and greenschist, if= iron formation. White areas are lakes.

4.2 Laboratory Data

Of 127 oriented L-S tectonite hand samples, 35 were selected for 55 thin sections for petrography, miscrostructural kinematic analysis and quartz petrofabric analysis. Selected samples represent the KSZ in length, width and lithology (Plate 1).

4.2.1 Petrography: Metamorphic Facies and Grade

Metamorphic mineral assemblages, deformation mechanisms, and quartz slip systems provide clues about metamorphic conditions that accompanied deformation. The metamorphic mineral assemblages of 55 thin sections, representing 35 rock samples, indicate that the rocks experienced amphibolite (Hbld + Plag ± Grt) and greenschist (Chl + Alb+ Ep/Czo + Qtz ± Act) facies metamorphism (Winter, 2000) (Plate 2). Mineral assemblages of 21 and 15 samples indicate amphibolite facies and greenschist facies metamorphism, respectively; one sample indicates either greenschist or amphibolite facies metamorphism (Plate 2). Amphibolite facies assemblages generally reflect lower amphibolite facies; garnet does not occur in any samples, although it was noted in outcrop at location KS8I.

Mineral microstructural features agree with greenschist to amphibolite facies and low to medium grade metamorphism. Undulose extinction of quartz, and feldspar internal microfracturing (Plate 3, e, sample KS6U1) indicate low to medium grade metamorphism, consistent with greenschist to amphibolite facies metamorphism (Passchier and Trouw, 2005). Quartz c-axis LPO diagrams indicate activity along the basal slip system, consistent with low to medium grade dynamic metamorphism; those results are reported in detail in section 4.2.2.

4.2.2 Le type: stretching vs. rolling

Kinematic indicators occur in a plane oriented with respect to the Le type (*rolling Le* or *stretching Le*, Fig. 8). Asymmetries will occur in the motion plane, which is Fm-perpendicular and *stretching* Le-parallel or Fm-perpendicular and *rolling* Le-perpendicular (Fig. 8). Eleven samples were cut in both Le-parallel and Le-perpendicular planes. Fm-perpendicular, Le-perpendicular planes dominantly (in nine of 11 rock samples cut in both Le-parallel and Le-perpendicular sections) lack asymmetry, whereas the Fm-perpendicular, Le-parallel plane dominantly shows asymmetry (Table 3, Fig. 18). Samples KS6U1 B and KS9K A are the two exceptions. Sample KS6U1 B, a Le-perpendicular section, has asymmetry in the Le-perpendicular plane (Table 3). Sample KS9K A, another Le-perpendicular section, might have asymmetry in the Le-perpendicular plane (Table 3). Asymmetric fabrics occur in Fm-perpendicular, Le-parallel planes (Fig. 18). Therefore, Le lie within the motion plane, and form normal to the vorticity axis. These relationships are consistent with non-coaxial shear with Le forming parallel to shearing.

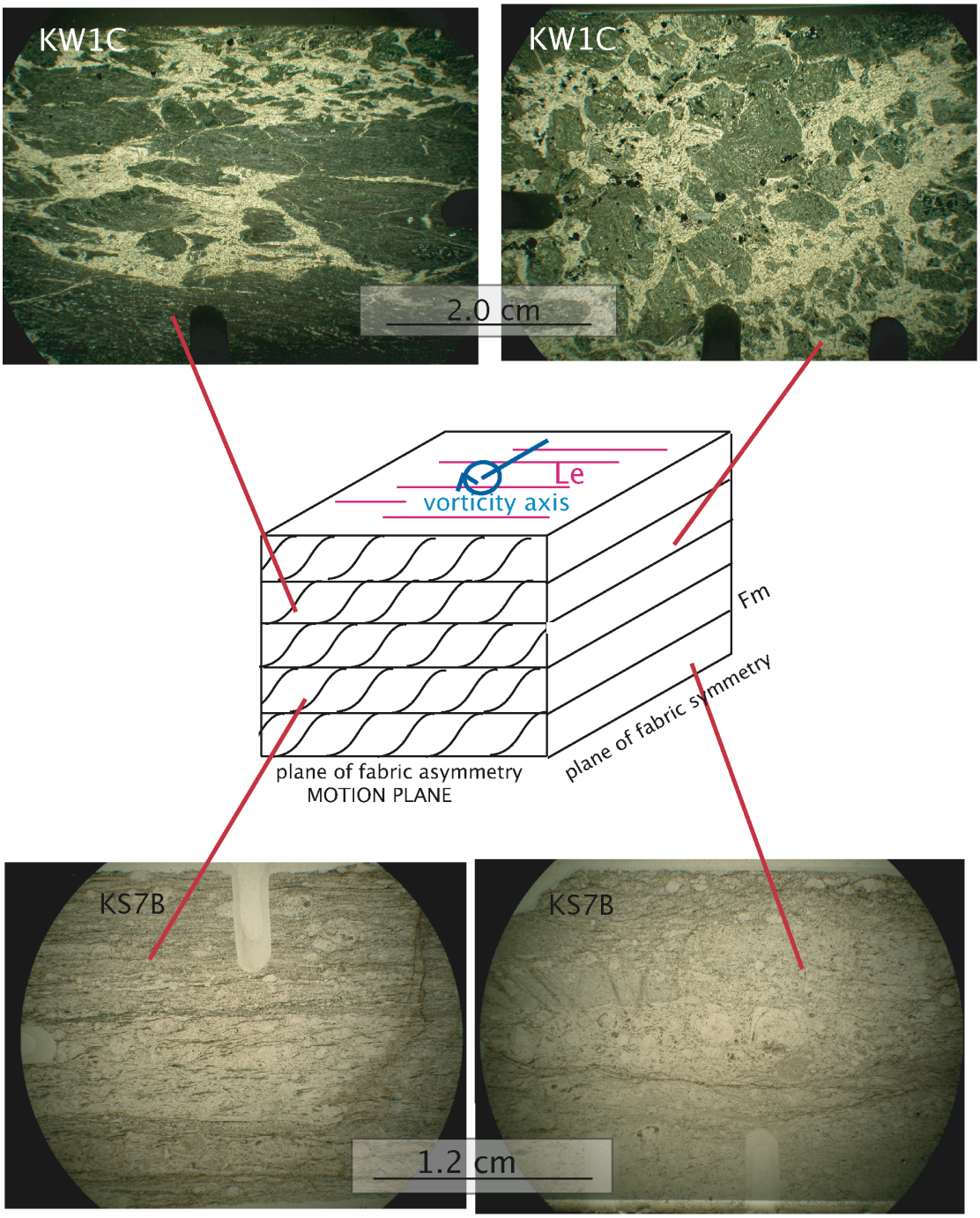

Figure 18. Le-perpendicular vs. Le-parallel plane views of samples KW1C and KS7B show asymmetry in the Le-parallel (motion plane) view and symmetry in the Le-perpendicular view.

4.2.3 Microstructure Analysis: Deformation and Kinematic Indicators

The deformation of the KSZ rocks is markedly ductile. Evidence for this includes: 1) ductile shear zone geometries (Fig. 13), 2) ductile deformation microstructures such as S-C fabric, grain shape preferred orientation, porphyroclast systems and sigmoids (reported below in this section), and 3) quartz LPO (reported in Section 4.2.4). Although brittle fractures and slickensides occur locally in the field, field and thin section samples of L-S tectonites lack evidence of brittle deformation such as fractures from cataclasis, gouge, and breccia. Evidence for intracrystalline deformation includes undulose extinction, microkinks, deformation lamellae and quartz LPO. Undulose extinction indicates cooling accompanied deformation. Quartz LPO indicates dislocation creep deformation (or crystal plastic deformation) where migration of vacancies to dislocation lines displaces a dislocation, allowing the dislocation to climb over a blocked site (Passchier and Trouw, 2005).

In metabasites, deformation at low grade conditions leads to continuous or spaced foliations defined by the preferred orientation of amphibole, chlorite, epidote, mica and lenses of different composition; mechanical growth is more important than solution transfer. At medium to high grades, oriented mineral growth and crystal plastic deformation control foliation development (Passchier and Trouw, 2005). KSZ Fm are defined by the preferred orientation of amphibole, chlorite, epidote, and mica. KSZ Le are formed by the preferred orientation of elongate monocrystalline minerals, typically micas, actinolite, or hornblende, and object lineations also include the preferred orientation of polycrystalline objects, typically chlorite, epidote or calcite.

Within the motion plane, shear sense indicators included S-C fabric, grain shape preferred orientation, porphyroclast systems and sigmoids (strain shadows, sigmoids, delta and sigma objects), fold asymmetry, and quartz LPO girdles. The dominant kinematic indicators used in this study are S-C fabric, grain shape preferred orientation, and porphyroclast systems and sigmoids (Plate 3). I ranked all kinematic interpretations with a confidence value from low (one) to high (five) confidence (Table 3).

S-C fabric consists of C-type shear band cleavage and S-planes. Continuous S-planes define a shape or mineral foliation that is cut by spaced distinct C-type shear band cleavage or C-planes (Passchier and Trouw, 2005). The C-type shear bands parallel shear zone boundaries. S-planes parallel the maximum directions of extension and internal strain axes, X_i, and Y_i, respectively. S-C fabric is the most robust kinematic indicator in this study (Plate 3). In granitoid sample KS6A, the chlorite (dark green) defines the S-foliation; some chlorite grains are more sigmoid than others (Plate 3a). Sigmoids are aggregates of grains of a mineral in a matrix of another mineral, lacking a clear porphyroclast core. Discrete zones of chlorite and epidote concentrations form fine and linear spaced C-planes in sample KS6U. The left-lateral shear sense shown in the KS6U photomicrograph indicates dextral strike-slip shear sense in geographic coordinates. Greywacke or volcaniclastic sample KS7J-c hosts continuous actinolite and hornblende that define S-planes and discrete zones (some marked with opaque Fe-oxide or epidote concentrations) that mark C-planes (Plate 3b). The right-lateral shear sense in the photomicrograph indicates dip-slip north-up shear sense in geographic coordinates. Intermediate volcaniclastic rock or tuff sample KS7C-b, hosts continuous biotite that defines S-planes and spaced discrete zones of biotite and epidote define C-planes (Plate

3-c). The right-lateral shear sense in the photomicrograph indicates north-up dip-slip shear sense in geographic coordinates. Orthogneiss sample KS9K-b hosts continuous biotite and epidote that define S-planes and discrete spaced zones of biotite and epidote define C-planes (Plate 3d). I gave each of these samples a confidence of five.

Porphyroclast rotation and associated tails also record shear sense. Rigid porphyroclasts can also accentuate an S-plane of an S-C fabric. Samples KS7C-b and KS9K-b (Plate 3c and d) show rigid-body feldspar and aggregate quartz (Plate 3h) rotations with associated sigma-shaped tails.

Grain shape preferred orientation (GSPO) describes a fabric of elongate mineral grains or subgrains. GSPO is not the same phenomena as a LPO of platy minerals, such as micas. Rather, GSPO fabric results from deformation of a set of ideally-spherical mineral grains with isotropic rheological properties. Deformation-produced GSPO mimics the geometry of the strain ellipse, with the long and short axes of the deformed grain parallel the maximum elongation axis (X_i) and minimum elongation axis (Z_i) of the finite strain ellipse, respectively (Plate 3e and f). The maximum elongation axis (X_i) of a geometric strain ellipse, which is oblique to the dominant spaced foliation plane of the samples, parallels the elongate quartz. In granitoid KS6U1, the long axis of quartz grains (X_i), aligns from the upper left to the lower right of the photomicrograph indicating left-lateral shear sense, which translates to dextral strike-slip shear sense in geographic coordinates (Plate 3e). I gave this sample a confidence of five. For sample KS7J, the long axis of quartz (X_i) aligns from the upper right to the lower left of the photomicrograph indicating right-lateral shear sense, which translates to north-up dip-slip

shear in geographic coordinates; the shear sense agrees with that indicated by the S-C fabric within the same sample and I gave the sample a confidence of five (Plate 3b).

Coarse-grained salvages in metabasalt rock KN8E are another sigma-shaped object that can indicate shear sense (Plate 3g and j). The coarse-grained salvages also resemble asymmetric shearband boudins, which can occur in sedimentary or tectonic layering and can occasionally give shear sense (Passchier and Trouw, 2005). I give sample KN8E a confidence level of four, not five, because the coarse-grained salvages or shearband boudins are the only shear sense indicator.

Mantled porphyroclasts consist of a central single crystal and a surrounding fine-grained mantle of the same mineral. The mantle can deform into wings (or trails) that extend on both sides of the porphyroclast and 'grow' in the X_i-direction of finite strain; the asymmetry reflects shear sense. Volcaniclastic rock KS3D hosts actinolite mantled porphyroclasts (Plate 3i). The mantles are wide near the porphyroclast, and mantle wings taper to the upper left and lower right of the photomicrograph forming a sigma shape. The sigma-type asymmetry fabric indicates left-lateral shear sense, north-up dip-slip shear in geographic coordinates. The mantled porphyroclasts of this sample predominantly gave left-lateral shear sense so I gave a confidence of four. The asymmetry, an imaginary line from the upper left to the lower right mantle in the photomicrograph, is also the long axis (X_i) of the instantaneous strain ellipse.

Several samples with steeply plunging Le give inconsistent or unreliable shear sense indicators (Table 3). Metabasalt sample KN3AAC is one example with inconsistent shear sense indicated by filled fractures (Plate 3k and Table 3). The fractures or veins open and new minerals grow parallel to the direction of least strain, the direction of

maximum instantaneous extension (Z_i). The fractures form and fill in at least two directions.

Overall, S-C fabric is the most robust shear sense indicator, especially where combined with other shear sense indicators. Other indicators such as GSPO, strain shadows, porphyroblast or rigid body rotations, vein fill, and coarse-grained salvage geometry were used as indicators when they indicate a consistent shear sense throughout the sample. I rated 16 samples from low (one) to high (five) confidence. I rated three samples one or two, and 13 from three to five (Table 3).

Shear sense was interpreted for 16 locations from examination of 55 thin sections. Four of 16 locations record south-up dip-slip, five record north-up dip-slip, one records east-up dip-slip, two record west-up dip-slip, and five record dextral strike-slip (Tables 3 and 4); one of the strike-slip locations also displays north-up asymmetry in the Le-perpendicular plane. Five of 55 samples display asymmetry in Le-parallel sections, but the shear sense is inconclusive (Table 3). Of the Le-perpendicular sections that have asymmetry in the Le-perpendicular plane, KS6U1 B and KS9K A, only KS6U1 B had a discernible, interpreted shear sense of north-up dip slip (Table 3). Although sample KS6U1 B only displays a shallow Le, nearby rocks (e.g. sample KS6J) display a steep Le. Of the 12 locations with dip-slip displacement, the south-up displacement pitch ranges from 78 to 100; the north-up displacement pitch ranges from 85 to 100; the east-up displacement pitch is 65; the west-up displacement pitch values are both 93. From four locations, the strike-slip shear record is dextral with pitch values of 0 to 30; I assigned a kinematic confidence of five to these samples. My kinematic confidence ranges from one to five in the dip-slip samples. Spatially, samples record south-up dip-

slip in the area north of North White Iron Lake, north-up dip-slip in the North Kawishiwi River area east of Farm Lake (KS7 zone), and dextral strike-slip record along the eastern North Kawishiwi River and south of the KS6 zone granite body (Plate 4).

Table 4. Pitch bins, shear sense and kinematic confidence

Pitch Bin	# with shear sense	# South-side-up	# North-side-up	# East-side-up	# West-side-up	Dextral Shear	Kinematic Confidence
0-30, 180-150	4	0	0	0	0	4	5
51-75	1	0	0	1	0	0	3
131-105	1	1	0	0	0	0	3
76-104	10	3	5	0	2	0	1-5

4.2.4 *Petrofabric analysis: quartz c-axes*

Four samples (two Le-parallel and two Le-perpendicular) from three locations were evaluated for quartz LPO. Quartz c-axis orientations were measured using the U-stage and plotted on equal area, lower hemisphere stereoplots (Turner and Weiss, 1963) in the U-stage reference plane. Pole data was rotated into the fabric element reference space, either Le-parallel or Le-perpendicular, and ultimately into the motion plane view (Figs. 19 – 22). Resulting fabric asymmetry records shear sense. Petrofabric analysis of quartz c-axes for each of four samples from three locations produced results consistent with kinematic microstructure. Three samples show evidence of quartz basal slip systems, indicating low T deformation (Passchier and Trouw, 2005). One sample displays evidence of rhombohedral slip, expected to operate at medium to high temperature (Passchier and Trouw, 2005). This result is inconsistent with low to medium

metamorphic grade determined from the sample's mineral assemblage. However, given the deformation history of the rock, the apparent medium to high T rhombohedral slip system may be reconcilable with the low-grade metamorphic facies. The four samples are discussed in detail in below.

Sample KS7J has quartz LPO, indicating ductile deformation. The long axes of quartz GSPO define a continuous foliation (S). A sharp discontinuity between quartz grains defines a spaced foliation (C). The c-axis stereoplot displays a Type I crossed girdle inclined to S; the LPO is asymmetric with respect to S foliation, indicating non-coaxial shear (Fig. 19)(Passchier and Trouw, 2005). The vorticity axis is perpendicular to Le, which further establishes that Le formed due to stretching, and not due to rolling. The girdle inclined to S indicates asymmetric right-lateral shear, which corresponds to north-up dip-slip shear sense in geographic coordinates, consistent with microstructural kinematic indicators (Table 3). The shape of the girdle indicates slip along the basal <a> slip system indicative of low temperature (≤ 350 ºC) conditions during deformation. These results are consistent with greenschist to amphibolite facies, low-grade metamorphism indicated by the mineral assemblage (Passchier and Trouw, 2005). Therefore, deformation and metamorphism were concurrent. The presence of undulose quartz indicates that cooling likely accompanied deformation.

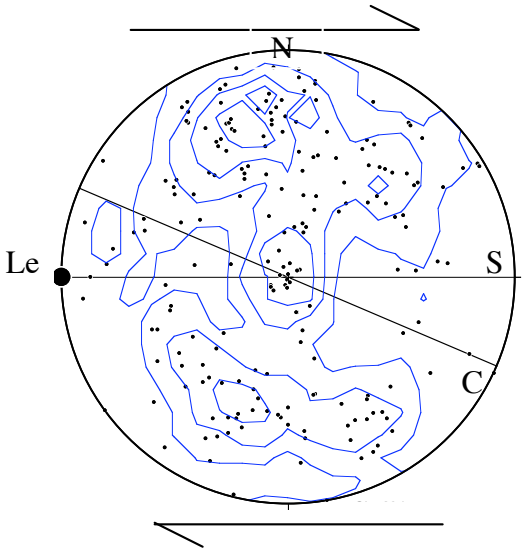

Figure 19. Sample KS7J quartz c-axes plot on equal area, lower hemisphere stereonet with Le, S and C foliations. This is a motion plane view of 200 points with Kamb contours (2σ statistical confidence interval) from an Le-parallel section. Arrows signify a right-lateral shear sense interpretation from the inclined girdle to S foliation.

Quartz LPO in samples KS8B-A and -B indicates ductile deformation. C-axes were measured in both Le-parallel (KS8B-B) and Le-perpendicular (KS8B-A) sections, and combined into a single motion plane view (Fig. 20). The long axis of quartz GSPO defines the S foliation. The basal slip system of points indicates low-T during deformation. The c-axes plot displays a Type-I crossed girdle inclined to S indicating north-up shear, consistent with microstructural kinematic indicators (Table 3). The girdle is perpendicular to the C foliation slip plane. A small quartz-layer fold runs through KS8B-B (Le-parallel section) and the quartz LPO is consistent throughout the fold. C-axes measured in both the Le-parallel and Le-perpendicular planes (rotated into the motion plane) show north-up shear sense (Fig. 21). Both c-axes plots are consistent with vorticity perpendicular to Le, indicating that Le formed via stretching rather than rolling. The population concentrations indicate slip along basal <a> consistent with low T

deformation, in agreement with greenschist metamorphic conditions determined from mineral assemblage, suggesting that deformation and metamorphism were concurrent. Quartz undulose extinction indicates that cooling accompanied deformation.

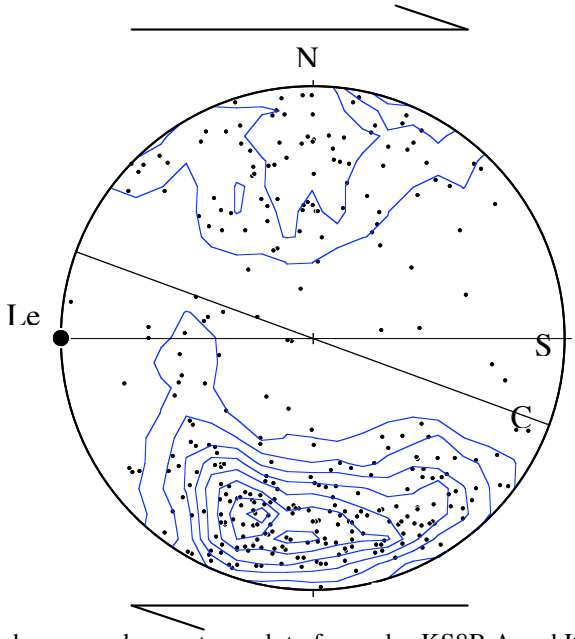

Figure 20. Lower hemisphere, equal area stereoplot of samples KS8B A and KS8B B quartz c-axes with Le, S and C foliations. Kamb contours shown with a 2σ statistical confidence interval. This is a motion plane view of 326 points from an Le-parallel section (n=200) and an Le-perpendicular section (n=126).

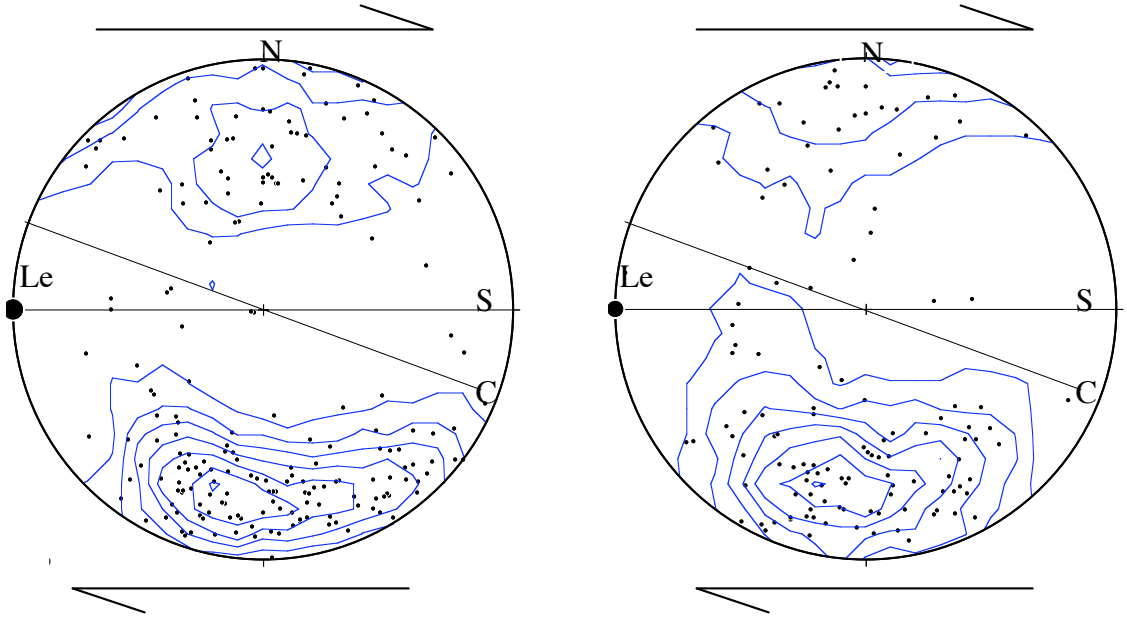

Le-parallel section data
(thin section KS8B B)

Le-perpendicular data rotated to Le-parallel view
(thin section KS8B A)

Figure 21. Lower hemisphere, equal area stereoplots of samples KS8B B and A quartz c-axes plot on equal area, lower hemisphere stereonets with Le, S and C foliations. Kamb contours shown with a 2σ statistical confidence interval. These two figures show the data from the Le-parallel section and the Le-perpendicular section (rotated into Le-parallel view). Arrows signify a shear sense interpretation from the inclined girdle to S foliation.

Sample KS6U displays a quartz c-axisLPO indicating ductile deformation. The long axis of quartz GSPO defines the S foliation. The c-axis girdle formed perpendicular to the slip plane or slip foliation C. The c-axis stereoplot shows a central population inclined toward S. The LPO is asymmetric with respect to the foliation, indicating non-coaxial shear (Fig. 22). The inclined data population gives a stereonet-view right-lateral shear sense, which corresponds to dextral strike-slip shear in geographic space, consistent with the shear sense interpreted from microstructural analysis (Table 3). The central population concentration indicates that the rhombohedral <a> and prism <a> slip system was active without basal <a> slip; the rhombohedral <a> to prism <a> slip systems indicate medium to high temperature during deformation (Passchier and Trouw, 2005).

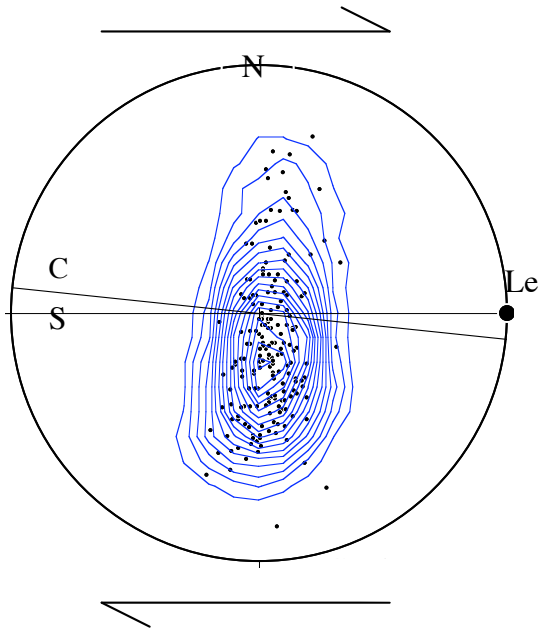

Figure 22. Lower hemisphere, equal area stereoplot of sample KS6U quartz c-axes with Le, S and C foliations. Kamb contours shown with a 2σ statistical confidence interval. This is a motion plane view of 200 points from an Le-perpendicular section rotated into Le-parallel section.

Medium T conditions could be inconsistent with greenschist to amphibolite facies metamorphic grade T. However, multiple deformation events are also consistent with the data. If the rock was initially homogeneous and isotropic, the first shear event would orient the c-axes. The other samples argue for slip along the basal plane. A second shear event would begin with those oriented slip systems, not a homogeneous and istotropic condition. A dip-slip shear event could orient random axes and then, a strike-slip shear event would re-orient those arranged quartz c-axes such that the *pseudo*-medium T rhombohedral <a> or *pseudo*-high T prism <a> population distribution occurs (Fig. 23). Moreover, undulose quartz in samples that record dip-slip shear indicates cooling, not heating, accompanied deformation. Oliver (1996) notes similar relationships in several greenschist facies shear zones.

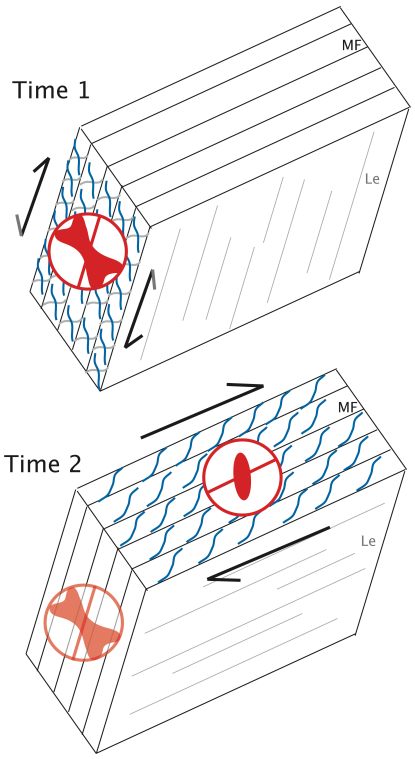

Figure 23. Block diagram illustrating the formation and re-activation of slip planes as quartz c-axes petrofabric forms in two stages, dip-slip deformation (time 1) with an unknown shear sense followed by dextral strike-slip deformation (time 2).

4.3 Summary of Data Results

The major results of this study are:

1. KSZ rocks experienced greenschist to amphibolite metamorphic facies conditions.
2. Fm trajectories are east-northeast in the greenstone, metavolcanic and metasedimentary rocks but varied and curving within the western Giants Range granitoid body of the KSZ.
3. Mineral lineations are stretching lineations. Asymmetries dominantly occur in the Le-parallel plane and the vorticity axis is normal to Le.
4. Steep pitch zones coinciding with dip-slip shear, are broad. Shallow pitch coincides with consistent east-west striking dextral shear in a focused zone.
5. The relative timing of two shear events is: 1) dip-slip displacement and 2) strike-slip displacement.

A compilation map of Fm trajectories, bedrock geology, pitch domains and kinematic results illustrates the geographic extent of the KSZ (Plate 4). The general extent of the KSZ is the zone along strike of the North Kawishiwi River presently known to contain L-S tectonites; following that definition, the KSZ is not only the narrow dextral strike-slip shear zone but actually a much wider zone that records dip-slip deformation as well. The presence of wetlands and glacial cover prohibit data collection in some areas of the KSZ region. The known extent of L-S tectonites shows that the KSZ is at least 3-5 km wide and steeply dipping; it has an average foliation of 075, 90, and a regionally dominant steeply-plunging Le as well as local gently-plunging Le. The KSZ steep dip-slip Le correspond with the broad (≥ 3-5 km-wide) steep pitch zones. The KSZ appears to be widest (≥ 5 km) in the west where the Knife Lake Group is widest. Volcanic, volcaniclastic, conglomerate, greywacke, and iron formation lithologies host the most obvious L-S tectonites whereas, pillowed basalt and granitoid rocks do not exhibit such a

pronounced L-S fabric. Ely Greenstone units (eg and egvd) typically lack Fm and Le, most likely, because basalt pillows serve to partition strain. Shallow strike-slip Le domains occur in a narrow, ~0.5 km-wide, zone of the KSZ. This narrow shear zone includes the area classified as the North Kawishiwi Fault (Green et al., 1966; Sims, 1976; Jirsa and Miller, 2004).

Kinematic and petrofabric data herein indicate that the more widely distributed dip-slip shear predates dextral strike-slip shear along a localized KSZ zone, as summarized in Fig. 24. Le orientation, metamorphic facies, kinematic and quartz petrofabric data all support a dip-slip shear event followed by a focused strike-slip shear event. Steeply oriented Le marks a broad zone of dip-slip deformation and shallow-plunging Le marks a narrow zone of strike-slip shear (Fig. 17 and Plate 4). Samples that record dip-slip shear display undulose quartz, indicating that cooling accompanied deformation. Dextral shear occurred in a narrow zone at a lower temperature or higher strain rate than dip-slip shear. Earlier dip-slip shearing resulted in oriented quartz LPO; later dextral shear, oriented 90° from the dip-slip shear, utilized the previously oriented basal <a> slip planes, creating a pseudo-rhombohedral <a> slip system in KS6U1 (Fig. 23). Dip-slip shear (with both north-up and south-up shear senses) occurred along steeply-dipping east-northeast-striking Fm, producing a regionally dominant down-dip Le. Granite doming produced curvate Fm trajectories in the western KSZ (Fig. 24). Subsequent dextral strike-slip shear focused along a narrow zone between the Ely Greenstone and the Giants Range Batholith granite, and within the Knife Lake Group volcanic rocks (Fig. 24). Younger events in the KSZ region include brittle deformation

(northeast-southwest striking faults and slickenside planes) and the Keeweenaw Intrusion in the southeast of the KSZ (Fig. 24).

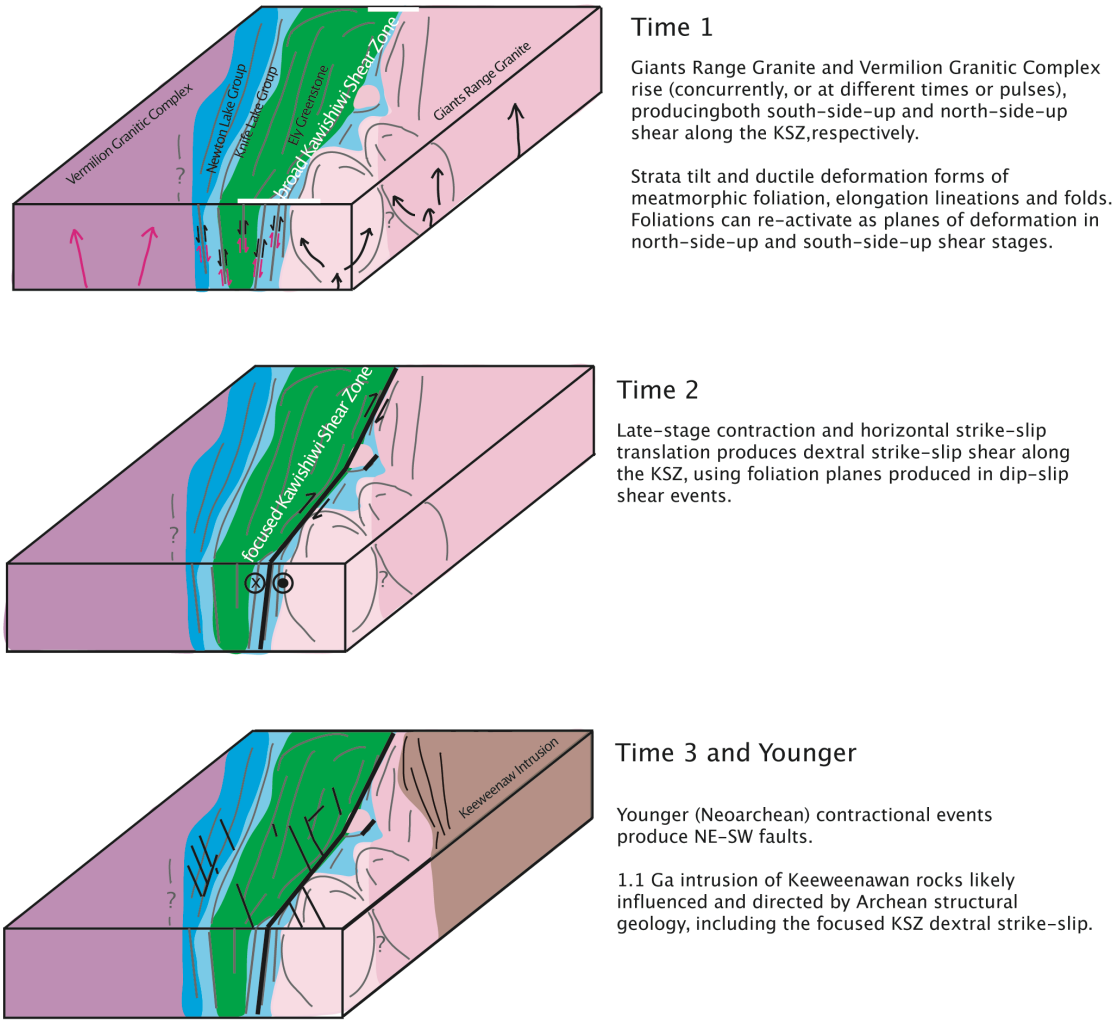

Figure 24.
Cartoon of block diagrams illustrating the two major deformation events recorded within the KSZ, in times 1 and 2. Younger events are combined in time 3.

5. Discussion

The KSZ structural and kinematic history includes at least two shear events: 1) one (or more) event marked by distributed dip-slip along a steeply-dipping east/northeast-striking zone and 2) a subsequent, spatially focused event of dextral strike-slip shear. Data presented herein favors the sagduction/diapirism hypothesis for this region of granite-greenstone terrain in the Superior Province, although it does not discount the arc-accretion hypothesis either. The data is consistent with work by, and includes that of, others (Green et al., 1966; Green and Shulz, 1982; Sims, 1976). My interpretations agree with those of Sims (1976) in particular. The results of this study warrant further study in the KSZ and in global granite-greenstone terrains; possible directions for future work are suggested.

5.1 KSZ Structural and Kinematic History

A first-order observation of the KSZ is the presence of both consistently east-northeast and curvilinear Fm trajectories. Fm trajectories trend consistently east-northeast within the Ely Greenstone, Knife Lake, and Newton Lake formations north of the KSZ and in the eastern Giants Range granitoid body southeast of the KSZ. The Giants Range granitoid of the KSZ hosts curvilinear Fm trajectories around North White Iron Lake, northern Farm Lake and South Farm Lake, respectively, and around an isolated granite body in the center of the KSZ. Curvilinear Fm trajectories suggest there was doming or local ballooning pulses of granitoid diapirism within the Giants Range granitoid.

In small-scale regional map view, the Giants Range granitoid bedrock geology, mapped without Fm trajectories, would appear to form a rather sharp east-striking contact with the units to the north; however, Fm trajectories do not follow this contact. Regions within the KSZ with curving Fm trajectories show spatial correlation with granite bedrock, which also dictate the rounded morphology of lake basins: North White Iron Lake, northern Farm Lake, South Farm Lake, and around the KS6 zone granite body.

This work establishes the regional mineral lineation as stretching Le. Le formed parallel to the motion plane and normal to the vorticity axis, consistent with non-coaxial shear with Le parallel to shear axis. It cannot be argued therefore, that the KSZ records predominant dextral strike-slip shear (with Le forming normal to the shear direction). Dextral strike-slip shear did, indeed, occur within the KSZ, however dextral shear occurred late within a spatially focused zone.

Structural and petrofabric analysis establish the relative timing of KSZ deformation events. Le domain, kinematic analysis, and quartz LPO analysis support two deformation events within the KSZ, dip-slip shear followed by dextral strike-slip shear. The bimodal Le distribution, with distributed steep Le cross-cut by focused shallow Le indicates the shear events along the KSZ. The diffuse dip-slip occurred first (as cooling progressed) followed by focused dextral strike-slip in that subsequent cooler and/or higher strain-rate rheological setting.

Sample KS6U1 has a shallow Le with asymmetries in both Le-parallel and Le-perpendicular planes, each with a confidence of five. This same sample hosts the rhombohedral slip plane for quartz c-axes rhombohedral slip plane. Taken together, this evidence also strongly suggests that dip-slip shear predated strike-slip shear.

Furthermore, nearby sample KS6J has a steep-Le, and records north-up shear. These samples from region KS6 border a local granite body within Knife Lake group rocks (Fig. 10, Plates 1and 4).

One might expect that south-up shear would be the predominant dip-slip direction in the KSZ because the Giants Range Batholith is directly to the south. However, the data include both north-up and south-up shear within the KSZ. Both north-up and south-up kinematic results require a mechanism of dip-slip deformation that could produce a varied dip-slip shear sense.

Petrologic arguments indicate that deformation accompanied metamorphism. The KSZ greenschist and dominant amphibolite facies metamorphic facies results are consistent with other granite-greenstone terrains and data from KSZ (Green, 1970; Sims, 1976). Granite-greenstone terrains typically have greenschist to amphibolite facies metamorphism with the higher-grade amphibolite facies occurring next to granite bodies, as in the KSZ.

5.1.1 *Implications for Hypotheses*

Results of this study are most consistent with the sagduction/diapirism hypothesis. The low to medium grade conditions observed are *possible* in either hypothesis, yet are inconsistent with crustal thickening predicted by the arc-accretion hypothesis. Curvilinear Fm trajectories suggest there was doming or local ballooning pulses of granitoid diapirism within the Giants Range granitoid, and are most consistent with the sagduction/diapirism hypothesis. The arc-accretion hypothesis predicts consistent, planar Fm trajectories but the sagduction/diapirism hypothesis predicts Fm trajectories that

curve around granite margins. Dip-slip shear is most consistent with the sagduction/diapirism hypothesis. Both sagduction/diapirism and arc terrane accretion hypotheses predict regional strike-slip shear. In the arc terrane accretion hypothesis, strike-slip shear occurs perpendicular to the convergence direction of accreting terranes along unit contacts. In the sagduction/diapirism hypothesis, strike-slip shear occurs in the end stage of the density-driven sagduction of greenstones and rising of granitoid bodies. Rising granitoid bodies expand and converge causing a crustal scale lateral flow accommodated by localized strike-slip shear zones (Rey and Houseman, 2006). If the buoyancy-derived stress were greater in the Archean, then lateral escape (strike-slip faults and crustal-scale lateral crustal flow) rather than large-scale thrust and thickening may have become the primary response to tectonic convergence.

5.1.2 *Implications for Other Regional Work*

The results of this study are inconclusive. They are most consistent with the sagduction/diapirism hypothesis, yet they cannot discount the arc-accretion hypothesis. My KSZ interpretation agrees with the interpretations of Sims (1976), and disagrees with the broader *interpretations* of much other work in the broader Vermilion District that favors the arc terrane accretion hypothesis or the Alogoman orogeny (Card, 1990; Green, 1970; Bauer and Bidwell, 1990; Jirsa et al., 1992).

Sims (1976) suggested that the Vermilion and Giants Range magmas rose into the volcanic-sedimentary pile; as they neared the surface the granitoid bodies would have expanded due to decreased lithostatic pressure and possibly inflation from new magma pulses. The rise and "mushrooming" of the granite would produce a compressive stress

on the volcanic-sedimentary pile leading to folding and contemporaneous metamorphism. The Vermilion Granitic Complex lies approximately 12 km to the north of the KSZ; the rise of this body could produce north-up dip-slip shear.

Based on stratigraphic unit offsets, Sims (1976) suggested that the dextral horizontal displacement along the Vermilion-Wolf Lake-North Kawishiwi Fault is 17 to 19 km. If true, it follows that present-day N-S transects across the KSZ would not represent relations prior to the dextral strike-slip displacement. Prior to offset, the Snowbank Lake granite would have been located in the central KSZ where the local granite body exists today. KS6U1, which preserves quartz c-axis and kinematic indicator evidence of dip-slip and dextral strike-slip shear, samples this body.

Sims also attributed major Vermilion District fold orientations to the rise and expansion of the Giants Range and Vermilion Complex granitoid bodies. On a regional scale, traces of isoclinal folds in supracrustal rocks are sub-parallel to the margins of the flanking Vermilion Granitic Complex and Giants Range granitoid and to the outer margin of the generally massive Ely Greenstone metabasalt (Sims, 1976). Isoclinal folding probably resulted from contraction caused by the relative upwelling and converging of the flanking granitoids (Hooper and Ojakangas, 1971; Sims, 1976), a mechanism consistent with the relatively low strength of the crust in the Archean thermal regime, and as predicted by diapir modeling (Ramberg, 1967).

Although Sims (1976) favored the sagduction/diapirism hypothesis, results and interpretations from other studies in the Vermilion District also support the sagduction/diapirism hypothesis. Hooper and Ojakangas (1971) attributed regional folds with step vertical axial planes to diapiric rise of the Vermilion Granitic Complex and

Giants Range granitoid. Bauer and Bidwell (1990) conclude that major structural features of the Vermilion District and southeastern Vermilion granitoid body are consistent with northwest-directed shortening. Rey and Houseman (2006) assert that regional shortening can occur as an end-stage in the sagduction/diapirism process. Masters theses structural and kinematic analyses of the Vermilion District Shagawa Lake Shear Zone and Mud Creek Shear Zone (Fig. 2) show dominant dip-slip deformation along these steeply-dipping east/northeast-trending shear zones within the Vermilion District (Erickson, 2008, and Karberg, 2008). These works document north-up dip-slip shear followed by south-up dip-slip shear, interpreted as the result of rising Vermilion and Giants Range granitoid bodies, respectively.

Summative work (e.g. Card, 1990) and secondary literature on Northeastern Minnesota granite-greenstone terrain geology (e.g. Minnesota Geological Survey website publications for the general public) typically invoke the arc-accretion hypothesis. This structural and kinematic study on the KSZ shows that the sagduction/diapirism hypothesis has yet to be discounted, but can not discount the arc-accretion hypothesis either.

5.2 Global Relevance of this Study: Granite-Greenstone Terrain Comparisons and Future Work

This study examined one shear zone within an Archean granite-greenstone terrain. The context of this greenstone belt must be considered within the larger context of a whole granite-greenstone terrain. In order to further address hypotheses for granite-greenstone terrain formation in the Superior Province, research could focus on the deformation and geothermobarometry within and near the granitoid bodies.

In a global comparison of granite-greenstone terrains, the scale and geometry of granite-greenstone terrains is important. In map view, the granitoid domes of the Pilbara granite-greenstone terrain stand out (Fig. 26a). In other granite-greenstone terrains, the Fm trajectories within granitoid bodies can reveal a similar geometry that is otherwise indistinguishable by a mapview of bedrock geology units alone (Fig. 26 b, c, d). The Pilbara (Fig. 26, a) and Yilgarn (Fig. 26d) of Australia and the Rhodesian craton (Fig. 26b) granite-greenstone terrains formed by sagduction and diapirism (Van Kranendonk and Collins, 1998; Van Kranendonk et al., 2003; Dalstra et al., 1998; Macgregor, 1951). Fm trajectories define the Yilgarn Ghooli *Dome* Complex (Fig. 26d). The Ghooli Dome Complex bedrock geometry, from north to south, is in fact reminiscent of Superior Province greenstone belt bedrock geometry from east to west. Further study in Superior Province granitoids could first, identify Fm trajectories. If Fm trajectories are curvate, one could then assess the global granite-greenstone terrain range of size of granitoid domes with-respect-to the width of greenstone-volcanic-sediment packages. For example, the western KSZ has curvate Fm boundaries that are only about one-fourth the diameter of those of the Yilgarn (Fig. 26, e). Yilgarn granitoid domes approximately

equal the diameter of the Pilbara domes but are smaller than some of the Rhodesian Craton granitoid bodies. If a scale-dependent pattern emerges, it would likely identify scale (or range in scale) of sagduction/diapirsm tectonic processes, which could be important if we are to understand why and how modern-style arc-accretion processes evolved. If the Superior Province represents one of Earth's youngest granite-greenstone terrains, then the scale of processes might be very different from Earth's oldest granite-greenstone terrains.

a) Pilbara Craton Domes (from Van Kranendonk et al., 2004)

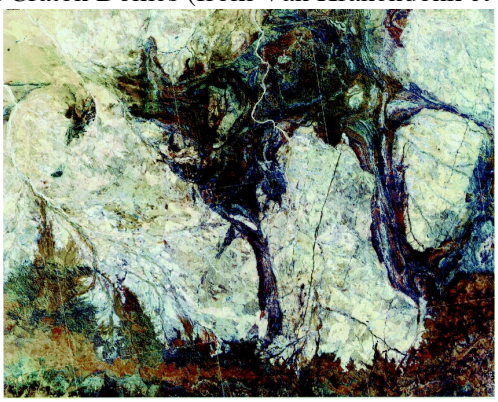

25 km

b) Rhodesian Craton

c) Superior Province

(from MacGregor, 1951)

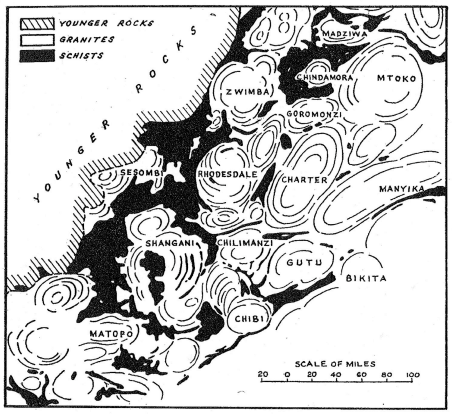

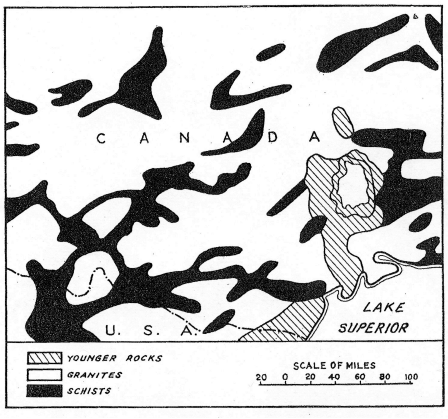

d) Yilgarn Craton (from Dalstra et al., 1998)

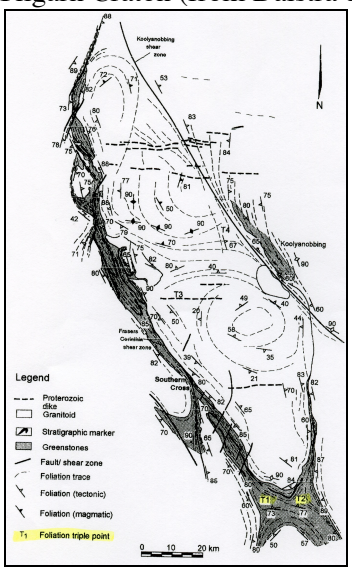

Figure 26. Maps of granite-greenstone terrains and granite Fm trajectories. a) Pilbara Craton, b) Rhodesian Craton, c) Superior Province, d) Yilgarn Craton. Granitoid bodies shown in white (or gray in a.), greenstone belts shown in black.

I recognized that my ability to distinguish between magmatic fabrics and metamorphic deformation in granite was limited, but the curvate Fm trajectory results within the Giants Range granitoid warrant further work. Determination of the emplacement mechanism of granitoid bodies in greenstone belts is fundamental for our understanding of the tectonic history of granite-greenstone terrains. Future work might follow the methodology of Dalstra et al. (1998) and Chardon et al. (2002) to determine the emplacement depth and mechanism of granitoid emplacement. Their methods include: structural geology, domain mapping, petrography and electron microscopy to determine stable mineral parageneses and mineral chemistry, granite U-Pb zircon age dates to determine timing of crystallization and geothermobarometry on granitoid mineral assemblages and xenoliths to find the depth of emplacement of granitoids. Chardon et al. (2002) mapped discrete shear zones in gneiss and granitoid rocks and performed U-Pb geochronology to constrain ages within several regions of the granitoid rocks. Further analysis of quartz c-axis petrofabrics would also be valuable, and perhaps best facilitated with electron backscatter diffraction (EBSD) technology.

Age dates specific to different regions of the Giants Range granitoid body, and other granitoid bodies in granite-greenstone terrains might illuminate various stages of crystallization and doming within apparently continuous granite batholiths. However, caution must always be paid to crystallization dates. If a granitoid body rises diapirically and deforms in solid-state, a crystallization date can predate diapirism. Improved age dating techniques could re-evaluate and possibly better constrain Superior Province and Vermilion District age dates.

Future work cannot discount the importance of structural domains when invoking an Archean tectonic process. Yet, structural domains and kinematic history must be paired with other geologic tools to better constrain the Archean geotectonic processes that formed granite-greenstone terrains.

6. Summary and Conclusions

The structural and kinematic data from the KSZ as described herein has spoken to the debate between granite-greenstone terrain formation by arc-accretion or sagduction/diapirism processes. The KSZ experienced regional dip-slip deformation likely associated with the rise of the Vermilion Granitic Complex and the Giants Range granitoid. Focused dextral strike-slip occurred as a later event along the KSZ, and perhaps caused by ballooning of the expanding granitic bodies. The data are consistent with Archean greenstone package sagduction and granite diapirism processes, although this data, alone, does not discount the arc-accretion hypothesis. This study indicates that continued work in Superior Province granite-greenstone terrains is warranted in order to elucidate those processes that formed some of Earth's earliest crust.

7. Bibliography

Anhaeusser, C.R., Mason, R., Viljoen, M.J., Viljoen, R.P., 1969. A reappraisal of some aspects of Precambrian shield geology. Geol. Soc. Am. Bull. 80, 2175-2200.

Arth, J.G. and Hanson, G.N., 1974. Geochemistry and origin of the early Precambrian crust of Northeastern Minnesota. Geochim. Et. Cosmochim. Acta. 39, 325-362.

Bauer, R.L. and Bidwell, M.E., 1990. Contrasts in the response to dextral transpression across the Quetico-Wawa subprovince boundary in northeastern Minnesota. Can. J. Earth Sci. 27, 1521-1535.

Bédard, J.H., Brouillette, P., Madore, L., and Berclaz, A., 2003. Archaean cratonization and deformation in the northern Superior Province, Canada: an evaluation of Plate tectonic versus vertical tectonic models. Precambrian Res. 127, 61-87.

Bjornerud, M., 2005. *Reading the Rocks: The Autobiography of the Earth*. Westview Press, Cambridge.

Burke, K. and Kidd, W.S.F., 1978. Were Archean continental geothermal gradients much steeper than those of today? Nature. 272, 240-241.

Card, K.D., 1990. A review of the Superior Province of the Canadian Shield, a product of Archean accretion. Precambrian Res. 48, 99-156.

Cawood, P.A., Kroner, A., Pisarevsky, S., 2006. Precambrian Plate tectonics: criteria and evidence. GSA Today. 16, 4-11.

Chardon, D., Peaucat, J-J., Jayananda, M., Choukroune, P., and Fanning, C.M., 2002. Archean granite-greenstone tectonics at Kolar (South India): Interplay of diapirism and bulk homogeneous contraction during juvenile magmatic accretion. Tectonics. 21, 7-1 – 7-17.

Collins, W.J., Van Kranendonk, M.J., Teyssier, C., 1998. Partial convective overturn of Archaean crust in the east Pilbara craton, Western Australia: driving mechanisms and tectonic implications. J. Struc. Geol. 20, 1405-1424.

Czeck, D.M. and Hudleston, P.J., 2003. Testing models for obliquely plunging lineations in transpression: a natural example and theoretical discussion. J. Structural Geol. 25, 959-982.

Dalstra, H.J., Bloem, E.J.M; Ridley, J.R.; Groves, D.I. 1998. Diapirism synchronous with regional deformation and gold mineralization, a new concept for granitoid emplacement in the Southern Cross Province, Yilgarn Craton, Western Australia. Australian Journal of Earth Sciences 46, 765-784.

Engel, A.E.J., 1968. The Barberton Mountain Land: Clues to the differentiation of the Earth. Geol. Soc. S. Afr.. 71, 255-270.

Erickson, E., 2008. Structural and Kinematic Analysis of the Shagawa Lake shear zone, Superior Province, northeastern Minnesota: Implications for Archean (2.75 Ga) Crustal Evolution. Masters thesis, University of MN Duluth.

Fowler, C.M.R., 2005. *The Solid Earth*. 2nd ed. Cambridge University Press, Cambridge.

Gee, R.D., 1979. Structure and tectonic style of the Western Australia shield. Precambrian Research 92, 327-369.

Green, J.C., 1970. Lower Precambrian Rocks of the Gabbro Lake Quadrangle, Northeastern Minnesota. MNGS. SP-13, 1-96.

Green, J.C., Phinney, W.C., Weibler, P.W. 1966. Geologic Map of Gabbro Lake Quadrangle, Lake County, MN. MNGS: M-2, scale 1:31,680.

Green, J.C., and Shulz, K.J. 1982. Geologic Map of the Ely Quadrangle, Lake and St. Louis Counties, Minnesota. MNGS. M-50, scale 1:24,000.

Hansen, V.L., 1990. Collection and preparation of thin sections of oriented samples. J. Geol. Ed. 38, 294-297.

Hallimond, A.F., 1970. *The Polarizing Microscope*. 3rd ed. Vickers Ltd., York.

Harland, W.B., 1971. Tectonic transpression in Caledonian Spitsbergen. Geol. Mag. 108, 27-42.

Hooper, P.R. and Ojakangas, R.W., 1971. Multiple deformation in Archean rocks of the Vermilion District, Northeastern Minnesota. Can. J. Earth Sciences. 8, 423-434.
Jahn, Bor-ming and Murthy, V.R., 1975. Rb-Sr ages of the Archean rocks from the Vermilion district, northeastern Minnesota. Geochim. Cosmochim. Acta, 39, 1679-1689.
Jelsma, H.A. and van der Beek, P.A., 1993. Tectonic evolution of the Bindura-Shamva greenstone belt (northern Zimbabwe): progressive deformation around diapiric batholiths. J. Structural Geol. 15, 163-176.
Jirsa, M.A. and Boerboom, T.J., 2003. Bedrock Geology of the Vermillion Lake 30' x 60' Quadrangle, Northeast Minnesota. MNGS, M-141, scale 1: 100,000.
Jirsa, M.A. and Miller Jr., J.D., 2004. Bedrock Geology of the Ely and Basswood Quadrangles, Northeast Minnesota. MNGS, M-148, scale 1: 100,000.
Jirsa, M.A., Southwick, D.L., Boerboom, T.J., 1992. Structural evolution of Archean rocks in the western Wawa subprovince, Minnesota: refolding of precleavage nappes during D_2 transpression. Can. J. Earth Sci. 29, 2146-2155.
Karberg, S., 2008. Structural and Kinematic Analysis of the Mud Creek Shear Zone, Northeastern Minnesota: Implications for Archean (2.75 Ga) Tectonics. Masters thesis, University of MN Duluth.
Kearey, P. and Vine, F.J. 1996. *Global Tectonics*. Blackwell Science Ltd., Oxford.
Kimura, G., Ludden, J.N., Desrochers, J-P., Hori, R. 1993. A model of ocean-crust accretion for the Superior Province, Canada. Lithos 30, 337-355.
Konopasek, J., Kroner, S., Kitt, S.L., Passchier, C.W., Kroner, A., 2005. Oblique collision and evolution of large-scale transcurrent shear zones in the Kaoko belt, NW Namibia. Precambrian Res. 139-157.
Kusky, T.M. and Polat, A., 1998. Growth of granite-greenstone terranes at convergent margins, and stabilization of Archean cratons. Tectonophysics. 305, 43-73.
LaBerge, G.L., 1994. *Geology of the Lake Superior Region.* Penokean Press, Oshkosh. 313 p.
Lambert, R. St. J., 1980. The thermal history of the Earth in the Archean. Precambrian Res. 11, 199-213.
Lin, S., 2005. Synchronous vertical and horizontal tectonism in the Neoarchean: Kinematic evidence from a synclinal keel in the northwestern Superior Craton, Canada. Precambrian Res. 139, 181-194.
Lin, S., Jiang, D., 2001. Using along-strike variation in strain and kinematics to define the movement direction of curved transpressional shear zones: An example from northwestern Superior Province, Manitoba. Geology. 29, 767-770.
Lin, S., Percival, J.A., Skulski, T., 1996. Structural constraints on the tectonic evolution of a late Archean greenstone belt in the northeastern Superior Province, northern Quebec (Canada). Tectonophysics. 265, 151-167.
Macgregor, A.M., 1951. Some milestones in the Precambrian of Southern Rhodesia. Transactions of the Geol. Soc. of South Africa. 54, 27-71.
Mareschal, J.C., West, G.F., 1980. A model for Archean Tectonism. Part 2. Numerical models of vertical tectonism in greenstone belts. Can. J. Earth Sci. 17, 60-71.
Moller, A. et al., 1995. Evidence of a 2 Ga Subduction Zone: Eclogites in the Usagaran Belt in Tanzania. Geology. 23, 1067-1070.
Mueller, W.U., Daigneault, R., Mortensen, J.K., Chown, E.H., 1996. Archean terrane docking: upper crust collision tectonics, Abitibi greenstone belt, Quebec Canada. Tectonophysics. 265, 127-150.
Oliver, Douglas, 1996. Structural, Kinematic and Thermochronometric Studies of the Teslin Suture Zone, South-Central Yukon Territory. PhD dissertation, Southern Methodist University, TX.
Passchier, C.W., 1997. The fabric attractor. J. Structural Geol. 19, 113-127.

Passchier, C.W. and Trouw, R.A.J., 2005. *Micro-tectonics*. 2nd ed. Springer, Berlin.
Percival, J.A. and Skulski, T., 2000. Tectonothermal evolution of the northern Minto Block, Superior Province, Quebec, Canada. Can. Mineral. 38, 345-347.
Ramberg, H., 1981. *Gravity, Deformation and the Earth's Crust*. 2nd ed. Academic Press, London.
Rey, P.F. and Houseman, G., 2006. Lithospheric scale gravitational flow: the impact of body forces on orogenic processes from Archaean to Phanerozoic. Geol. Soc. London. 253, 153-167.
Rey, P.F., Phillippot, P., and Thebaud, N., 2003. Contribution of mantle plumes, crustal thickening and greenstone blanketing to the 2.75-2.65 Ga global crisis. Precambrian Res. 127, 43-60.
Robin, P.F. and Cruden, A.R., 1994. Strain and vorticity patterns in ideally ductile transpression zones. J. Struc. Geol. 16, 447-466.
Schulz, K.J., 1980. The magamatic evolution of the Vermillion greenstone belt, NE Minnesota. Precambrian Res. 11, 215-245.
Sengupta, S. and Ghosh, S.K., 2004. Analysis of transpressional deformation from geometrical evolution of mesoscopic structures from Phulad shear zone, Rajasthan, India. J. Structural Geol. 26, 1961-1976.
Sims, P.K., 1976. Early Precambrian tectonic-igneous evolution in the Vermillion district, northeastern Minnesota. Geol. Soc. Am. Bull. 87, 379-389.
Sims, P.K., Reed Jr., J.C., Bickford, M.E., Houston, R.S., Link, P.K., Rankin, D.W., Van Schmus, W.R., 1993. Precambrian: Conterminous U.S. *The Geology of North America* Vol. C-2. Geol. Soc. America, Boulder.
Stanley, S.M., 2005. *Earth System History*. 2nd ed. W.H. Freeman and Co., New York.
Tabor, J.R. and Hudleston, P.J., 1991. Deformation at an Archean subprovince boundary, northern Minnesota. Can. J. Earth Sci. 28, 292-307.
Tarney, J., Dalziel, I., Dewit, M., 1976. Marginal basin 'Rocas Verdes' complex of S. Chile: a model for Archaean greenstone belt formation. In Windley, B.F. (ed). *The Early History of the Earth*. Wiley, London, p. 131-46.
Turner, F.J. and Weiss, L.E., 1963. *Structural Analysis of Metamorphic Tectonites*. McGraw-Hill, Inc., New York.
Twiss, R.J. and Moores, E.M., 1992. *Structural Geology*. W.H. Freeman and Co., New York.
Unzog, W. and Kurz, W., 2000. Progressive development of lattice preferred orientations (LPOs) of naturally deformed quartz within a transpressional collision zone (Panafrican Orogen in the Eastern Desert of Egypt). J. Structural Geol. 22, 1827-1835.
van der Pluijm, B.A. and Marshak, S., 1997. *Earth Structure*. McGraw-Hill, U.S.A.
Van Kranendonk, M.J., 2004. Preface Archaean Tectonics 2004: A Review. Precamb. Res. 131, 143-151.
Van Kranendonk, M.J., Collins, W.J., Hickman, A., Pawley, M., 2003. Critical tests of vertical vs. horizontal tectonic models for the Archaean East Pilbara Granite-Greenstone Terrane, Pilbara Craton, Western Australia. Precambrian Res. 131, 173-211.
Wahlstrom, E.E., 1979. *Optical Crystallography*. 5th ed. John Wiley and Sons, New York.
Wiebe, R.A. and Collins, W.J., 1998. Depositional features and stratigraphic sections in granitic plutons: implications for the emplacement and crystallization of granitic magma. J. Structural Geol. 20, 1273-1289.
Windley, B.F. 1984. *The Evolving Continents*. 2nd ed. Wiley, London.

8. Appendix

Table 1. Hypothesis Predictions- Expanded Version

	ARC TERRANE ACCRETION Also referred to as: "**Mobilist or Plate Tectonic**" (Windley, 1977) "**Actualistic Model**" (Rey, Chardon et al., 2002) "**Horizontal tectonics**" (Lin, 2005; Van Kranendonk et al., 2003) "**Uniformitarian** view" (Kearey and Vine, 1996)	**SAGDUCTION / DIAPIRISM** Also referred to as: "**Fixist or Classical**" (Windley, 1977) "**Vertical tectonics**" (Lin, 2005; Van Kranendonk et al., 2003; Bedard et al, 2003) "**Non-uniformitarian view**" (Kearey and Vine, 1996)
Shear zone distribution	Discrete distribution of shear zones b/c cool and brittle and strong Granites and/or greenstones record shear	Diffuse distribution of shear zones b/c weak (hot, low pressure) Solid-state granitoid bodies can flow, typically do not record shear; greenstones record shear
Younging and Age Relations	Younging direction across "order of accretion" with youngest region closest to subduction Time of terrane collision is marked by the maximum age either of cross-cutting intrusives or of sediments unconformably overlying both terranes (Twiss and Moores, 1992) Imbrication could displace or repeat the order	No significant difference in age of granitoid bodies vs. greenstones required; should be no younging direction, but there might be stages of sagduction and diapirism. Granitoid bodies could young to the center (Rey, pers. comm., 2007) No terranes of distinct age and/or origin
Displacement/ kinematics	Fold-and-thrust belts because cold and brittle Transpression possible Apparent polar wander (APW) paths of terranes are different, until collision and suture, than single APW (Twiss and Moores, 1992) Deformed suture region with strike-slip faults	Limited fold-and-thrust belts because ductile; ductile deformation Transpression possible Granitoid bodies move up, greenstones move down
Strain Distribution	Strain localization along linear belts (Rey, 2006)	Distributed strain
Elongation lineation (Le)	Uniform (possible variation in initial formation) (could be parallel or perpendicular to fold axes) (Twiss and Moores, 1992)	Multiple orientations; shallow toward top and steep towards center of greenstone; progressive change of orientation away from granitoid bodies

Le and foliations	Orientations: Consistent Lee, specifically fold hinge lineations parallel to regional distribution of fold hinges (Twiss and Moores, 1992); Elongation lineation consistent along strike normal transects Consistent foliations perpendicular to convergence direction and contraction; Uniform and along lines perpendicular to convergence (follow fold axial trace and other brittle displacements)	Orientations: Range of lineations, specifically around the granitoid; Elongation lineation orientations normal to granite boundary, thus orientations radiate around round granitoid bodies Foliations more broad Foliations mimic/parallel granitoid boundaries Curving mimics granitoid boundaries (steep on margins, shallow on surface)
Metamorphic Facies *Normal gradient (w/ increasing depth) is:* Chlorite Biotite Garnet Kyanite Sillimanite	Different metamorphic facies, specifically, greenstones have higher grade than granites High P, various T due to thrusting Could get inverted metamorphic zones during thrusting Highest-grade rocks underlie central portions of orogenic belt, unmetamorphosed rocks on flanks High grade→ coarse foliation and highly metamorphosed tectonites	Greenschist facies away from granite plutons to amphibolite facies at margins along granites Could get inverted metamorphic zones during diapirism Low grade→schistosity and crenulation cleavage
Seismic data	Expect subduction signature of slabs with higher velocity	Lack velocity change along "slab plane"
Folds	Thrust faults, nappes likely Uniform vergence Displacement direction transverse to the orogenic belt in outer areas of thrust nappes; shear direction is parallel to the axis of the orogenic belt in central orogenic core (Twiss and Moores, 1992)	Various vergence directions (especially in greenstones between granitoids), thrust faults if brittle (maybe over granitoids)
Granite plutons	Are remnant dehydration rising diapers, now exposed by erosion (Bedard, 2003) Plutons emplaced in cold, rigid country rocks and would undergo less penetrative tectonic strain than in sagduction/diapirism; plutons would preserve the kinematics of magma flow into the growing pluton	Are emplaced by density-driven rise Emplacement deformation and rise occurs in solid-state Crystallization ages could be older than emplacement ages (or younger if low T cooling occur)
Response to Convergence	Large-scale thrust faults and thickening (Rey, 2006)	Lateral escape: strike-slip faults, crustal-scale lateral flow (Rey and Houseman, 2006)

Table 2. Grain-scale deformation processes for some minerals

1. quartz -with increasing water pressure in the pore space, dislocation creep strength decreases -at very low grade conditions: brittle, pressure solution, solution transfer (fractures in grains, undulose extinction, kink bands) -at low-grade: dislocation glide and creep (patchy and sweeping undulose extinction, deformation lamellae) -at med. temps(400-550 ºC): dislocation creep, prism slip {m}<a>, recovery and recrystallization (SGR), pressure solution, old grains may be completely replaced by recrystallized material -at 500-700 ºC: GBM recrystallization, lobate grain boundaries, pinning or migration structures -above 770 ºC: prism slip {m}<c> , rapid recovery and recrystallization→strain free appearance, lobate grain boundaries, square subgrain structure (chessboard extinction or chessboard subgrains)
2. calcite and dolomite -v. low grade: deforms by fracturing and cataclastic flow, coarser-grained fragments heavily twinned and show undulose extinction, cut by veins and stylolites; small matrix grains can be strain- and twin free -low grade: if water present then pressure solution is dominant in calcite→ stylolite development. Calcite special! b/c twins from diagenesis onwards; can twin at room temp. (but dolomite does not twin below 330 ºC); dolomite is usu. stronger than calcite → boudinage of dolomite layers in a calcite matrix -low-med. grade: grain boundary sliding and superplastic behavior may be important in calcite if the grain size is very small -calcite and dolomite twin on different planes
4. feldspars -Plagioclase and K-feldspar deform similarly -deformation is strongly dependent on metamorphic condition -several dislocation slip systems can be active (esp. at high T) -low grade (below 400 ºC): brittle fracturing and cataclastic flow (bent cleavage planes and twins, patchy undulose extinction, subgrains with vague boundaries) -low-med. grade: internal microfracturing + minor dislocation glide (tapering deformation twins, bent twins, undulose extinction, deformation bands and kink bands with sharp boundaries)(flame-shaped albite lamellae could be in K-spar) -med. grade: dislocation climb possible, recrystallization (BLG)→ mantle structures, cataclastic failure→abundant microkinking -higher T: less twinning, myrmekite growth along crystal faces parallel to foliation, abundant flame-perthite in K-spar -high grade: dislocation climb and recovery are "easy", subgrain structures form, abundant myrmektite
5. micas -deform mainly by slip on either (001)<110> or (001)<100> -pressure solution, fracturing, undulose extinction, kinking and folding -folding occurs on the outside and pressure solution or kinking in the core of a folded crystal -fractures: assoc. w/ deflection of basal planes and lead to barrel or fish-shaped boudinaged grains -GBM important at med. to high grade -in brittle domain: biotite may show crude kinking or layer parallel slip to develop 'cleavage steps' or mica fish -muscovite is more resistant to deformation than biotite and forms mica fish in mylonite

6. olivine

-has different slip systems at different temperatures in the mantle
-old grains show strong undulose extinction and subgrain boundaries
-recrystallizes to fine-grained crystals that are concentrated in shear zones by flow partitioning
-a strong LPO and trails or bands of other minerals in olivine might be the only indication that it was deformed
-water may influence slip system (LPO with [001] max parallel to stretching lineation could be related to hydration rather than low T

7. orthopyroxene

-dislocation glide is dominant on (100)[001], but also has other slip systems
-dislocations usu. split into partial dislocations, separated by a stacking fault along which the crystal lattice is transformed into that of clinopyroxene, so exsolution lamellae of clinopyroxene can develop parallel to (100)
-at upper mantle conditions (up to 1000 ºC): may form ribbon grains with aspect ratios up to 100:1, equidimensional porphyroclasts if grains had an orientation that was unsuitable for slip
-ribbon grains form due to dominant (100)[001] slip system
-garnet, spinel, plagioclase or quartz can form exsolution lamellae on orthopyroxene

8. clinopyroxene

-has more slip systems than orthopyroxene
-At high T (>500 ºC) and/or low strain rate, multiple slip occurs
-does not easily form ribbons like orthopyroxene at high T
-garnet, spinel, plagioclase, hornblende or quartz can form exsolution lamellae in clinopyroxene

9. garnet

-at low grade: behaves as a rigid mineral, but lattice bending possible
-elongate lensoid and folded shapes of garnet crystals parallel to the deformation fabric subgrain structures and a LPO are found in some garnets = evidence for crystalplastic deformation
-at low-med grade: garnet is stronger than quartz and feldspar, but at higher temperatures all 3 minerals can deform together
-many slip systems can be activated, but one dominates 1/2<111>{110}
-ductile deformation can produce a LPO but garnet seems to have a weak preferred orientation in deformed rocks

10. amphiboles

-expect them to be stronger in ductile deformation than clinopyroxenes (b/c amphibole has longer Burger vector length), but opposite is true
-deformation behavior is poorly understood
-below 650-700 C: brittle deformation and dissolution-precipitation, and aggregates of fine-grained hornblende probably form by fracturing rather than dynamic recrystallization
-excellent cleavage on {110} planes → dominant brittle behavior
-at high T (above 700 ºC) and in dry rocks hornblende can deform by crystalplastic deformation
-at high T and/or low strain rate have several slip systems
-'garben' (German for "stack") = characteristic structure in hornblende schists = bundles of elongate hornblende crystals that are oriented in fan-like arrangements usually parallel to the foliation plane. 'Garben' may develop by growth of subgrains in the direction of the c-axis in previously deformed hornblende crystals.

Table 3. Definitive Mineral Assemblages of Metamorphic Facies for Mafic Rocks

Facies	**Definitive Mineral Assemblage in Mafic Rocks**
Zeolite	zeolites: especially laumonite, wairakite, analcime
Prehnite-Pumpellyite	prehnite + pumpellyite (+ chlorite + albite)
Greenschist	Chlorite + albite + epidote (or zoisite) + quartz ± actinolite
Amphibolite	Hornblende + plagioclase (oligoclase-andesine) ± garnet
Granulite	*Orthopyroxene* + clinopyroxene + plagioclase ± garnet ± hornblende
Blueschist	Glaucophane + lawsonite or epidote (+ albite ± chlorite)
Eclogite	Pyralspite garnet + omphacitic pyroxene (± kyanite)
Contact Facies	Mineral assemblages in mafic rocks of the facies of contact metamorphism do not differ substantially from that of the corresponding regional facies at higher pressure.

(from Winter, 2001; after Spear, 1993)

Appendix C.D. includes:

1. Plates: figures and tables listed in Table of Contents
2. GIS files

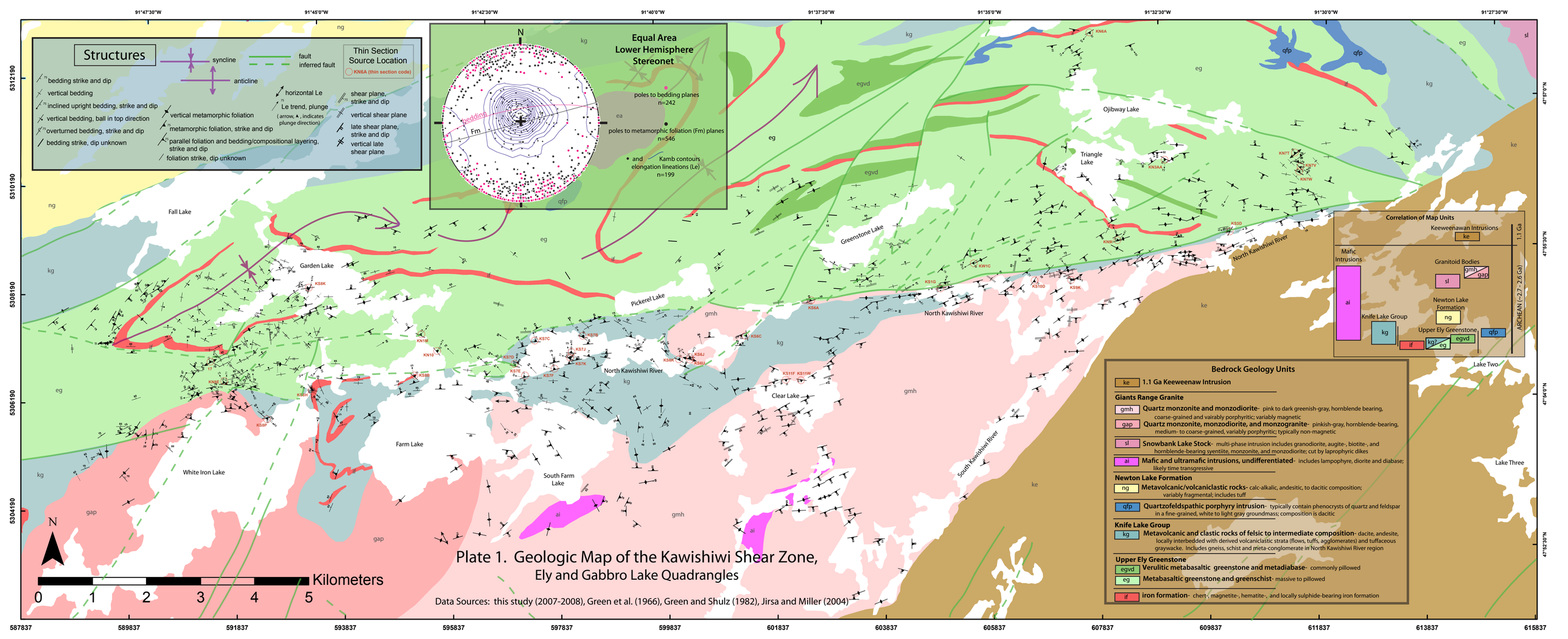
Structures
syncline
anticline
fault
inferred fault
bedding strike and dip
vertical bedding
inclined upright bedding, strike and dip
vertical bedding, ball in top direction
overturned bedding, strike and dip
bedding strike, dip unknown
vertical metamorphic foliation
metamorphic foliation, strike and dip
parallel foliation and bedding/compositional layering, strike and dip
foliation strike, dip unknown
horizontal Le
Le trend, plunge
(arrow, ▲, indicates plunge direction)
shear plane, strike and dip
vertical shear plane
late shear plane, strike and dip
vertical late shear plane
Thin Section Source Location
KN6A (thin section code)
Equal Area Lower Hemisphere Stereonet
poles to bedding planes n=242
poles to metamorphic foliation (Fm) planes n=546
and Kamb contours elongation lineations (Le) n=199
N
Fm
Bedding
Correlation of Map Units
Keeweenawan Intrusions
ke
1.1 Ga
Mafic Intrusions
Granitoid Bodies
gmh
gap
sl
ai
Newton Lake Formation
ng
Knife Lake Group
kg
Upper Ely Greenstone
qfp
if
kg?
egvd
eg
ARCHEAN (~2.7 - 2.6 Ga)
Bedrock Geology Units
ke 1.1 Ga Keeweenaw Intrusion
Giants Range Granite
gmh Quartz monzonite and monzodiorite- pink to dark greenish-gray, hornblende bearing, coarse-grained and variably porphyritic; variably magnetic
gap Quartz monzonite, monzodiorite, and monzogranite- pinkish-gray, hornblende-bearing, medium- to coarse-grained, variably porphyritic; typically non-magnetic
sl Snowbank Lake Stock- multi-phase intrusion includes granodiorite, augite-, biotite-, and hornblende-bearing syenitite, monzonite, and monzodiorite; cut by laprophyric dikes
ai Mafic and ultramafic intrusions, undifferentiated- includes lampophyre, diorite and diabase; likely time transgressive
Newton Lake Formation
ng Metavolcanic/volcaniclastic rocks- calc-alkalic, andesitic, to dacitic composition; variably fragmental; includes tuff
qfp Quartzofeldspathic porphyry intrusion- typically contain phenocrysts of quartz and feldspar in a fine-grained, white to light gray groundmass; composition is dacitic
Knife Lake Group
kg Metavolcanic and clastic rocks of felsic to intermediate composition- dacite, andesite, locally interbedded with derived volcaniclastic strata (flows, tuffs, agglomerates) and tuffaceous graywacke. Includes gneiss, schist and meta-conglomerate in North Kawishiwi River region
Upper Ely Greenstone
egvd Verulitic metabasaltic greenstone and metadiabase- commonly pillowed
eg Metabasaltic greenstone and greenschist- massive to pillowed
if iron formation- chert-, magnetite-, hematite-, and locally sulphide-bearing iron formation
Fall Lake
Garden Lake
Pickerel Lake
Greenstone Lake
Ojibway Lake
Triangle Lake
North Kawishiwi River
Clear Lake
Farm Lake
South Farm Lake
White Iron Lake
Lake Two
Lake Three
N
0 1 2 3 4 5 Kilometers
Plate 1. Geologic Map of the Kawishiwi Shear Zone,
Ely and Gabbro Lake Quadrangles
Data Sources: this study (2007-2008), Green et al. (1966), Green and Shulz (1982), Jirsa and Miller (2004)
91°47'30"W
91°45'0"W
91°42'30"W
91°40'0"W
91°37'30"W
91°35'0"W
91°32'30"W
91°30'0"W
91°27'30"W
47°57'0"N
47°55'30"N
47°54'0"N
47°52'30"N
5312190
5310190
5308190
5306190
5304190
587837
589837
591837
593837
595837
597837
599837
601837
603837
605837
607837
609837
611837
613837
615837

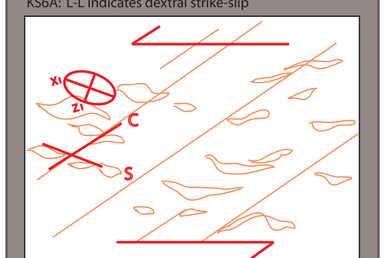

Confidence = 5

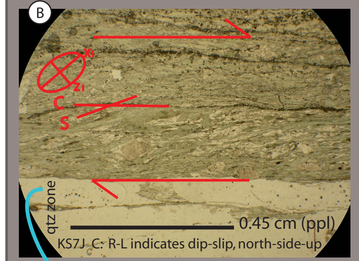

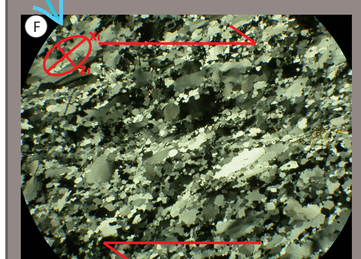

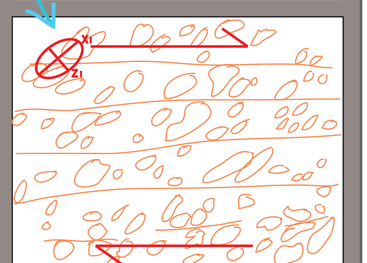

Confidence = 5

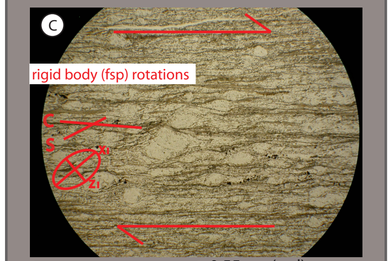

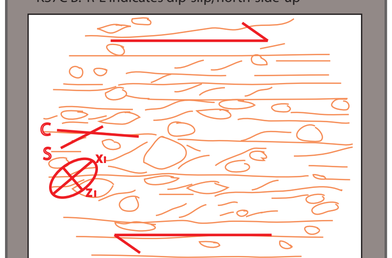

Confidence = 5

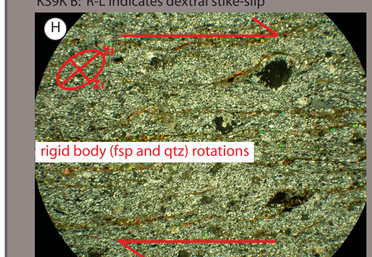

Confidence = 5

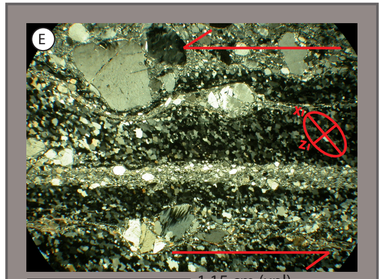

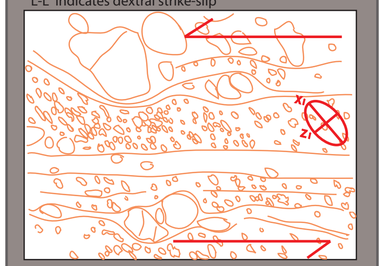

Confidence = 5

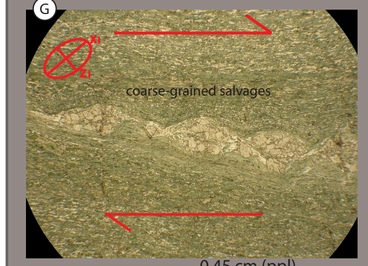

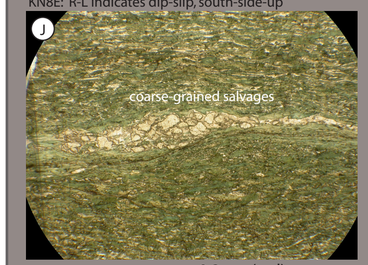

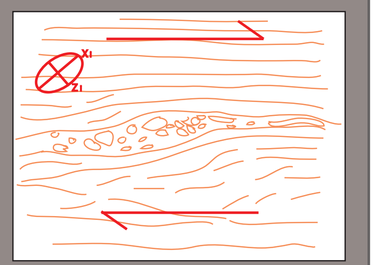

Confidence = 4

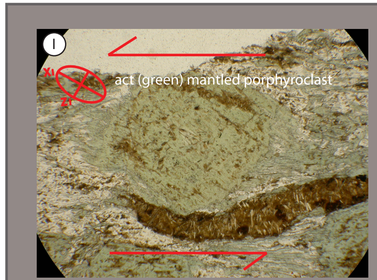

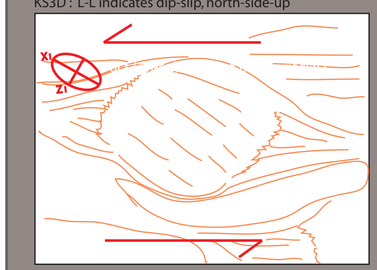

Confidence = 4

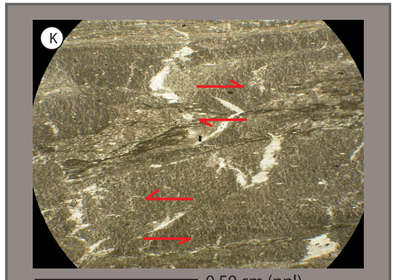

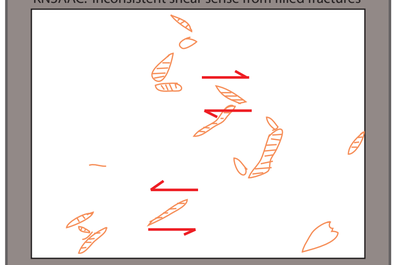

Photomicrographs and interpretations of Le-parallel, motion plane, views for shear sense indicators with respect to the instantaneous strain ellipse(box L). Shear sense indicators used in this study include S-C fabrics (A, B, C, D), grain shape preferred orientation (GSPO) (E, F), rigid body porphyroblast rotations (C, H), mantled porphyroclasts (I), coarse-grained salvages (J), and vein fill (K). Gray boxes enclose multiple photomicrographs from the same thin section.

Confidence value ranks the kinematic intrepretation from low confidence (1) to high confidence (5).

Plain polarized light (ppl), cross polarized light (xpl)

See Table 3 and Plate 2 for more kinematic and mineral assemblage information for samples shown here.

Plate 3. Kinematic Shear Sense Indicators

91°47'30"W 91°45'0"W 91°42'30"W 91°40'0"W 91°37'30"W 91°35'0"W 91°32'30"W 91°30'0"W

5312800 5310800 5308800 5306800 5304800 5302800 5300800 5298800

47°57'0"N 47°55'30"N 47°54'0"N 47°52'30"N 47°51'0"N 47°49'30"N

588433 590433 592433 594433 596433 598433 600433 602433 604433 606433 608433 610433 612433 614433

N

Folds
anticline
syncline

Fall Lake
Garden Lake
Pickerel Lake
North Kawishiwi River
Greenstone Lake
Ojibway Lake
Triangle Lake
Lake One
Clear Lake
Farm Lake
South Farm Lake
White Iron Lake
South Kawishiwi River

KS8K
KS8B b
KS7C b,c
KS7B
KS6J
KS6A
KN7T
KS3D
KS9K b,c
KS7J b,c
KS6U 1
KS7F
KS7K 2a
KN8E a,b
KN8F 1
KS8P 2

metamorphic foliation trajectories
Archean Rocks (2.7-2.6 Ga)
Keeweenawan Rocks (1.1 Ga)

Pitch Domains and Symbology

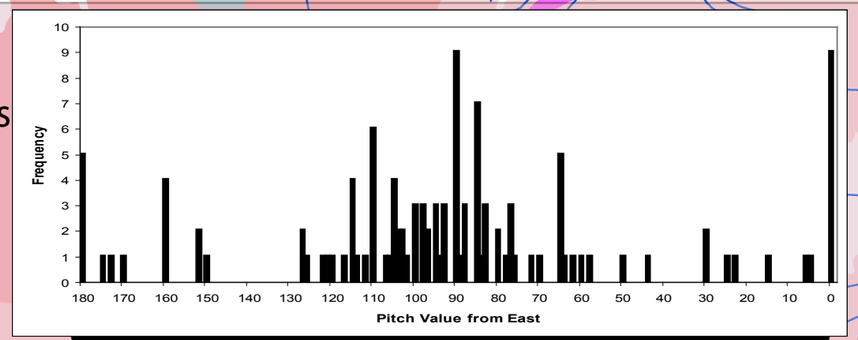

? = inferred pitch domain

Kilometers
0 2.5 5

SHEAR SENSE
Up
Down
north-up
south-up
strike-slip
Confidence Level
1 low
2
3
4
5 high

Bedding, Fm and Le

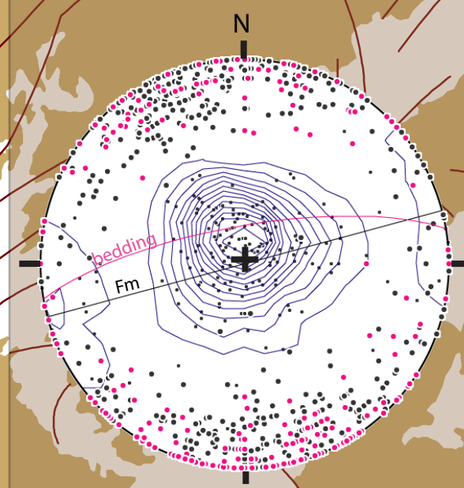

Equal Area
Lower Hemisphere
Stereonet

poles to bedding planes
n=242

poles to metamorphic foliation (Fm) planes
n=546

and Kamb contours
elongation lineations (Le)
n=199

Plate 4. Kinematic Results with Bedrock Geology and Foliation Trajectories